Detecting ASD in individuals based on their Brain Functional Connectivity Patterns

by

Md Mehedi Hasan
20301196
Samirah Dilshad Salsabil
24341094
K. M. Abul Farhad-Ibn-Alam
20301061
Prima Sarker
20301204

A thesis submitted to the Department
of Computer Science and Engineering in partial fulfillment of the requirements
for the degree of B.Sc. in Computer Science

Department of Computer Science and Engineering
Brac University
November 2024

Declaration

It is hereby declared that

1. The Final Thesis Report submitted is our own original work while completing the degree at Brac University.
2. The Final Thesis Report does not contain material previously published or written by a third party, except where this is appropriately cited through full and accurate referencing.
3. The Final Thesis Report does not contain material which has been accepted, or submitted, for any other degree or diploma at a university or other institution.
4. We have acknowledged all main sources of help.

Student's Full Name & Signature:

Md Mehedi Hasan	Samirah Dilshad Salsabil
20301196	24341094
K. M. Abul Farhad-Ibn-Alam	Prima Sarker
20301061	20301204

Approval

The thesis/project titled "Detecting ASD individuals based on their Brain FunctionalConnectivity Patterns " submitted by

1. Md Mehedi Hasan (20301196)
2. Samirah Dilshad Salsabil (24341094)
3. K. M. Abul Farhad-Ibn-Alam (20301061)
4. Prima Sarker (20301204)

Of Fall 2024, has been accepted as satisfactory in partial fulfillment of the requirement for the degree of B.Sc. in Computer Science on November 30, 2024.

Examining Committee:

Supervisor:
(Member)

Md. Golam Rabiul Alam, PhD
Professor
Department of Computer Science and Engineering
Brac University

Program Coordinator:
(Member)

Md. Golam Rabiul Alam, PhD
Professor
Department of Computer Science and Engineering
Brac University

Head of Department:
(Chair)

Sadia Hamid Kazi, PhD

Chairperson and Associate Professor
Department of Computer Science and Engineering
Brac University

0.1 Ethics Statement

We formally announce the outcomes of our research to be in favor of this concept. This study, in its whole, is devoid of plagiarism. The source material includes citations for any additional information sources. For the purpose of awarding a degree, this thesis has not been submitted, in whole or in part, to any other institution or organization.

Abstract

The main focus of this research is on accurate pediatric neurodevelopmental disorder diagnostics as well as early detection of Autism Spectrum Disorder (ASD) children and adolescents. Given the heightened neuroplasticity of the brain during these formative years, the ability to detect ASD (Autism Spectrum Disorder) early in development has profound implications for intervention and outcomes.This inherent variability poses a challenge when attempting to classify ASD (Autism Spectrum Disorder) using the intricate 4D fMRI data from ABIDE I that captures both spatial and temporal aspects of brain activity. Majority of research dealing with the neuroimaging methods has typically reduced this high-dimensional 4D data to a 2D correlation matrix, leading to a potential loss of crucial information related to both the dynamic brain activity and the connectivity patterns. In response to this limitation, we introduce an innovative preprocessing framework, NeuroSeg3D (Neuroimaging Segmentation for 3D framework), a cutting-edge pipeline designed to preserve the full 4D integrity of the fMRI(Voxel intensity) data. Also by retaining the inherent temporal and spatial complexities of the 4D fMRI scans, NeuroSeg3D empowers the model to extract a more nuanced understanding of the brain's architecture, which is paramount for accurate ASD classification. Building on this advanced preprocessing methodology, we developed CASD-Net (Children ASD Neural Network), a specialized convolutional neural network (CNN) meticulously engineered to handle the complexities of 4D neuroimaging data. CASD-Net (Children ASD Neural Network) utilizes state-of-the-art deep learning techniques to extract high-level features from raw fMRI volumes, capturing both spatial and temporal dependencies crucial for distinguishing ASD from non-ASD individuals. By employing multiple convolutional layers, attention mechanisms, and optimization strategies, CASD-Net(Children ASD Neural Network) is able to identify and learn intricate patterns within the 4D brain scans that are often imperceptible to conventional analysis methods. Beside this the model's performance was rigorously evaluated through both test set validation and 5-fold cross-validation, ensuring its robustness and generalizability across different subsets of data. Most importantly CASD-Net(Children ASD Neural Network) has achieved a remarkable test accuracy of 93.97%, underscoring its high performance in distinguishing ASD from control subjects. Beyond that, the cross-validation results of the model depicted a solid generalization capabilities, with an average accuracy of 83.57%, an average loss of 0.3147, and a standard deviation of 16.27%, and thus highlighting the model's adaptability despite variability in the dataset. The model we developed has demonstrated a robust performance through the classification metrics like precision, recall, and F1-score. Ensuring that both ASD(Autism Spectrum Disorder) and control classifications were accurate, reliable, and balanced. This result has underscored an enormous potentiality that our developed model possessed while revolutionizing neuroimaging diagnostics, especially with the complex and high-dimensional data ABIDE I.

Keywords: ASD, CNN, CASD-Net, NeuroSeg3D, Spatio-temporal, ABIDE, Neuroimaging, Segmentation, Voxel-intensity, 4-Dimensional-Data

Table of Contents

Chapter 1

Introduction

Human beings are naturally social beings and take cues from nature through language, emotions, and behaviors. However, people with Autism Spectrum Disorder (ASD), could be highly impaired since this is a complex neurodevelopmental disorder whereas individuals differ from typical peers based on the way they perceive the world and also based on how they interact with others. Symptoms and abilities in ASD can take various forms. This spectrum is usually diagnosed at an early age in childhood and characterized by the failure to respond to one's name, avoidance of eye contact, and repetition of certain behaviors. For now, without a known cure for Autism Spectrum Disorder(ASD), early diagnosis and intervention in the course of a disorder can help a child improve overall development and interaction with society. Specifically its fundamental diagnosis is related to the shortcomings in social interaction, conveying emotions, and behavioral facts. Actually, people with Autism Spectrum Disorder (ASD) most often underperform across at least some of these areas like- trouble communicating or socializing, as well as confined repeating patterns of behavior, anticipation, or interests [35]. However these areas are widespread and all people with Autism do not necessarily have the same behavioral pattern. Due to the complexity and wide spectrum behavior shown or portrayed by them, the diagnosis of this disorder is one of the most challenging, especially because of the overlapping features with other neurodevelopmental disorders [16]. To overcome these complications, researchers have begun to resort to advanced techniques like brain imaging techniques, including functional magnetic resonance imaging, to identify more objective biomarkers of Autism Spectrum Disorder (ASD). It inspects cerebral endogenous activity in accordance with fluctuations in oxygenation in the blood levels, allowing researchers to sketch out the neural networks of the brain while the individual is at rest. Despite this great promise of rs-fMRI, even traditional machine learning approaches, which have been the choice in various research, most of the time lack the discovery of subtle yet important relationships that could act like reliable biomarkers of Autism Spectrum Disorder (ASD). Furthermore to our initial approaches using traditional sequential model, several studies convert the 3D fMRI images with time series to correlation matrices within different regions-of-interest (ROIs) given by different atlases to classify ASD to neurotypical controls, [13], several of them reduce the temporal information [14]. However, such subjective feature selection techniques could significantly cause hindrance in detection of intricate patterns in neural activity, conceivably resulting in suboptimal outcomes. For the next phase of our methodology, we convert the 4D fMRI data into a dif-

ferent format that is customized for CASD-Net, our custom-built 3D CNN-based model specifically developed for analyzing volumetric neuroimaging data. This conversion is expedited by NeuroSeg3D, a preprocessing pipeline that includes temporal segmentation, reassembling and data normalization. These approaches ensure the optimal integration of fMRI data directly into the 3D CNN. In this process, we use a sliding window approach for temporal segmentation, while voxel resampling is used for spatial resolution standardization. We input the prepared fMRI data keeping the dimensionality essentially the same into CASD-Net, capturing both temporal and spatial patterns of brain connectivity efficiently. Moreover, the architecture of CASD-Net is designed for volumetric data analysis and in terms of learning complex multi-dimensional features, it surpasses traditional 2D CNN. The limitation of the ensemble spatiotemporal models as initial approach compelled us to switch our focus to CASD-Net architecture as our final proposed method, this study presents a progressive framework for early detection of ASD in individuals using fMRI data. Through providing an efficient as well as accurate, and unbiased diagnostic mechanism, this study not only anticipates in improving the probability of successful classification but also assists in restorative early intervention.

1.1 Motivation

Autism Spectrum Disorder (ASD) is a critical disorder as it is dependent on the critical brain connectivity patterns of individuals to identify. Therefore, for improving any development outcomes for this disorder, early detection becomes very crucial as it enables the necessary timely intervention, leveraging the neuroplasticity of the brain during childhood and adolescence. Additionally, these specific age groups of children and adolescence are critical periods of significant growth and reorganization in neural networks of brains. Studies show that the mean age of acquiring a diagnosis of ASD is 4 years 3 months and surprisingly, there has not been any significant changes over the past 2 decades despite the rigorous efforts to educate the public and medical professionals [11]. After the age of 18, the brain reaches a state that is more stable and developed. This makes it significantly harder to identify the developmental gaps caused by ASD, thus, delay in diagnosing until adulthood not only reduces the potency of interventions, but also limits the opportunities to improve one's quality of life and their ability to merge into the society [1]. With the challenges linked to behavioral and observational methods, neuroimaging techniques like fMRI hold expansion in possibilities, as it works as objective biomarkers that are not dependent on any external characteristics or subjective observation. In spite of the possibilities of fMRI, traditional analysis methodologies often cease to unveil the subtle but critical relationships in high-dimensional fMRI data. By focusing on children and adolescents, our research aims to amplify early detection efforts, by leveraging advanced methodologies to explore the intricate developing brain connectivity patterns.

1.2 Problem Statement

At the present time Functional MRI brain imaging (fMRI) has been identified as one of the most efficient and potential components for Autism Spectrum Disorder

(ASD) detection. In particular, studies have identified that the functional connectivity of people with Autism can be analyzed quantitatively to improve diagnosis accuracy further[18]. In addition to this diagnosis provides a non biased molecular framework to understand the distinctive levels of brain function in each individual. Moreover, fMRI apprehends spatiotemporal brain connectivity after measuring variations in blood oxygen levels. This eventually offers a quantitative and unprejudiced framework for understanding discrete brain functions. Although the fMRI data has immense prospective, the data are high-dimensional with complicated patterns, thus this poses significant challenges for traditional machine learning models to be able to recognize such complex networks of connectivity. Not to mention, nowadays the deep learning techniques, especially like 3D Conventional Convolutional Neural Networks (3D CNNs), Deep Neural Networks (DNNs),and Long Short-Term Memory Networks(LSTM), hold great promise for enhancing the diagnosis of ASD. Specially, 3D CNN has demonstrated exceptional prospects in medical imaging tasks, particularly the diagnosis of neurodevelopmental disorders. Likewise these models typically evade classical approaches as they are superior in uncovering intricate patterns and associations that typically evade classical approaches. Thus, they are theoretically well-suited to analyze the extensive information embedded in the fMRI datasets. Although there is quite a considerable amount of research that has validated the use of deep learning for ASD diagnosis, detailed and thorough studies exploring the performance of deep learning models in a systematic way in big datasets like the Autism Brain Imaging Data Exchange dataset are few and far between.

The main problem of the fMRI data is that the fMRI data captures brain activity over time in 3D spatial resolutions, resulting in large and complex datasets. This high dimensionality makes the data computationally intensive and difficult to analyze using traditional machine learning methods[13]. Moreover it can be affected by head motion during scanning, introducing motion artifacts that distort brain signals. While preprocessing methods, such as those provided by the Connectome Computation System (CCS), address these issues to some extent, the resulting data may still suffer from reduced quality, especially in the subtle connectivity patterns that are important for ASD diagnosis[3]. Furthermore fMRI signals have a naturally low signal-to-noise ratio, which makes it difficult to detect meaningful brain connectivity patterns. These complexities have reanimated the development of more robust machine learning models which are capable of handling such high-dimensional and noisy data.

1.3 Research Objectives

The main purpose of our research is to develop a robust model for detecting or classifying ASD based on the fMRI data. With our initial approach, we explored the ensemble of spatiotemporal models such as Convolutional Neural Networks (CNNs), Long Short-Term Memory Models (LSTM), Bidirectional LSTMs (Bi-LSTM), and Gated Recurrent Unit Networks (GRU) and while exploring we identified several limitations in the integration of the architecture. Hence, we transition to a more streamlined approach. Our aimed method is a 3D Convolutional Neural Network (CNN) based model, designed for volumetric feature learning. The emphasis of our approach is on the integration of spatial and temporal features within func-

tional brain data for capturing the complex connectivity patterns associated with ASD. This consolidated model captures those complex spatiotemporal patterns of fMRI data, which eliminates the necessity of separate spatial and temporal models. Moreover the approach of this model outputs into a single prediction mechanism may result in a more accurate and objective diagnostic method.

Our objective is to implement NeuroSeg3D as it is a prominent preprocessing pipeline that prepares 4D fMRI data via temporal segmentation, spatial normalization and voxel resampling. This pipeline establishes high-quality and standardized data for the deep learning models and preserves critical spatiotemporal information. Therefore, enhanced data quality will allow the models to extract critical biomarkers of ASD, while addressing limitations of traditional preprocessing techniques. This research aims to assess the performance of our model on the ABIDE dataset, while comparing it with the standard methods. This evaluation will provide validation to the capability of our model to accurately classify individuals with ASD and neurotypical controls, presenting with apprehensions of brain connectivity patterns. The outcomes will demonstrate our designed model as a definitive mechanism to diagnose ASD using volumetric neuroimaging data. Our study focuses on the fMRI data from children and adolescents to pinpoint ASD biomarkers during various critical stages of brain development. While early detection of ASD during childhood and adolescence maximizes the convenience of neuroplasticity, it also improves therapeutic outcomes and long-term quality of life. We believe that the ability of our model in analyzing pediatric brain connectivity patterns will certainly contribute to timely and effective clinical applications for ASD. Our research aims to establish our custom-tailored model as an impartial, automated and extensible diagnostic aid for ASD. In our work, we address the limitations of the hybrid models and traditional behavioral observations, as we aim to present such a model that offers a data-driven approach to simplify the diagnostic workflow. By enhancing the diagnostic precision, our goal is to enable ASD detection in clinical settings earlier and more reliably with our model.

1.4 Research Contribution

In our work, we present a novel approach to contribute to ASD detection on the basis of their brain connectivity patterns. As we propose a novel pipeline and model, this not only contributes by spatial and temporal brain connectivity patterns, but also by providing efficiency in detecting individuals with ASD from neurotypical controls.

- As the brain development patterns during adulthood are less complicated, we address the complexities of brain structure in children and adolescents. Our work particularly focuses on individuals of this age group for early detection of ASD. With the unique and crucial challenges related to their brain development, working on their fMRI data points out the intricate differences in the brain connectivity patterns between ASD and neurotypical controls.

- ABIDE I being a very complicated dataset to work with, the lackings in detailed and comprehensive documentation of the data has been evident. Given

the absence of detailed documentation of the data, we provide a coherent and comprehensive explanation of the data, which clarifies its structure, nuances and challenges. This is a critical contribution to the research that involves this dataset.

- In our work, to employ more advanced visualization techniques, we utilize Nilearn, facilitating a better understanding of the critical fMRI data. While dealing with large-scale high-dimensional fMRI data from ABIDE I, using Nilearn provides more insightful representation and analysis of brain connectivity patterns.

- With our work, we introduce NeuroSeg3D, a novel pipeline for fitting complex 4D fMRI data to a 3D CNN-based model. This method provides significant advancement by enabling the integration and makes room for more effective modeling and analysis on fMRI data. NeuroSeg3D provides a robust tool for future research as its technique is adaptable to any 4D fMRI dataset.

- With the aim of improving accuracy and efficiency in ASD detection using fMRI data, we propose CASD-Net, a novel 3D CNN-based architecture, particularly custom-designed for fMRI data. By leveraging advanced deep learning methods, this model enhances the performance of ASD detection. This model not only optimizes computational resources but also improves classification outcomes by focusing on both spatial and temporal brain connectivity patterns.

Chapter 2

Literature Review

2.1 Related Work

Cheruku Nagamani et al. (2024) prove an analysis on the effectiveness of different machine learning approaches to diagnose individuals with ASD. The authors use behavioral and social interaction screening data that are typically associated with ASD, which makes validation very vague, whereas using neuroimaging data like fMRI could provide more nuanced results of the study [45]. The study compares several machine learning models such as- SVM, Decision Tree, Random Forest, k-NN, where they achieved better outcomes from Random Forest and SVM in terms of accuracy. However, using deep learning techniques like DNN could provide higher accuracy as it could capture complex patterns more efficiently. The biggest challenge in this study was using less complex data and detecting ASD solely with a linear machine learning approach, as ASD is too complex to detect just by facial image or behavioral and social interaction.

Monisha Thomas and Aneesha Chandran (2018) provide a system by analyzing brain scans using Artificial Neural Networks (ANN) for diagnosing Autism Spectrum Disorder (ASD). With their approach they have integrated structural MRI (sMRI) and functional MRI (fMRI) data from ABIDE repository in order to classify individuals with ASD and neurotypical controls. They pre-process the structural features from Cerebral White Matter (CWM) and Cerebral Grey Matter (CGM) with Blood Oxygenation Level Dependant (BOLD) signals from fMRI using explicit techniques like slime time correction and Gray Level Co-occurrence Matrix (GLCM). Then, they feed these features into an ANN classification. To assess the corresponding effectiveness of ANNs in diagnosing ASD, the paper could interest from comparing its approach with other machine learning models such as Support Vector Machines (SVM) and Convolutional Neural Networks (CNN), even though the use of ANNs for combining the data of fMRI and sMRI shows potential. Due to individual variations in brain structures and activity patterns, the authors express challenges in generalizing the recognition system. This suggests that the classification accuracy could be improved with more advanced feature selection techniques. In spite of these challenges, important insights into the use of neuroimaging data for ASD detection is provided by this particular study. Moreover, this study highlights the prospects of ANN for improving early detection, but leaves space for future study of alternative techniques to increase reliability and performance in this realm [15].

Kyoungseob Byeon et al. (2020) propose a system that classifies Autism Spectrum Disorder (ASD) using resting-state functional magnetic resonance imaging (rs-fMRI) data with a novel Artificial Neural Network (ANN) model. To optimize feature extraction, the authors employ techniques like Orthogonal Least Squares and Orthogonal Subspace Pursuit were used in this approach. ABIDE I dataset has been used in this study, including rs-fMRI scans of individuals with ASD and neurotypical controls. The sensitivity rates between 73% and 93% were achieved by the system, which is considerably promising. However, the main challenge in this study was generalization of the system across individuals especially in noisy environments with diverse connectivity patterns, preaching the necessity of advanced noise separation techniques [20].

Carla Caballero et al. (2018) provide a study of the noise signatures of head motion data harnessed under different sampling resolutions which they extracted from resting state fMRI data [12]. In this study, the quality of the noise of the variability of the raw linear and angular speeds for various clinical phenotypes was distinguished in correspondence to age-matched controls. Besides, they approach modeling head motion characteristics over various clinical phenotypes. Moreover, the authors use bootstrapping methods for statistical comparison of compatible group sizes. The major challenge in this study is variability in sampling resolutions in the dataset, creating inconsistency in the research. Additionally, the residual noise created by head motion correction, could have a major impact in the reliability of the study on functional connectivity of ASD.

Jose O Maximo et al. (2021) provide a study on alterations in brain entropy in resting state functional MRI data in children with both ASD and neurotypical controls. The intention of this study is to contribute to entropy in children with ASD. The study uses Sample Entropy (SampEn) [28]. However, in order to capture subtle dynamic patterns, use of Permutation Entropy (PE) would give better outcomes. Additionally, Spearman ranks correlations with SampEn were used in order to test Social Responsiveness Scores (SRS) and brain-behavioral correlates. One of the key challenges in this study is the optimization technique on the ABIDE dataset, which lessens the credibility of the outcomes of ASD. Furthermore, the authors only focus on brain entropy which leave many relevant neural dynamics.

Seulki Yoo et al. (2024) provide a study on the asymmetric structural connectivity of the whole brain of individuals with ASD. The study uses the diffusion MRI from the ABIDE dataset to probe into the asymmetry index obtained from low-dimensional representation of structural connectivity where they portray weaker right-side dominance in individuals with ASD. The authors use supervised machine learning techniques like Support Vector Machines (SVM), Random Forest, Decision Trees etc to portray connectome asymmetry as a predictive measure for non-verbal communication of individuals with ASD. The major challenge of this study is it leans only on diffusion magnetic resonance imaging, leaving room for providing comprehensive understanding on ASD [46].

Subah et al. (2021) propose a model with the goal to classify ASD using fMRI data from ABIDE I dataset. The techniques used for preprocessing in this study are motion correlation, spatial smoothing and temporal filtering to remove noise and

then data is normalized to a standard Montreal Neurological Institute (MNI) space. After preprocessing, functional connectivity matrices were created and transformed into feature vectors. To learn patterns from each of the data, the authors use DNN to process connectromes from the atlases (CC200. AAL, BASC and Power) simultaneously [29]. The authors add two hidden layers to the DNN for classification. They use 80% of the data for training and 20% for testing. For ensuring a robust model evaluation, they opt for 5-fold cross-validation. The authors acquire 88% accuracy with BASC atlas. While the accuracy for their approach is significant, the study does not incorporate temporal dynamics of brain activity, which could improve the model performance.

Nicha C. Dvornek et al. (2017) introduce a study focused on Default Mode Network (DMN) to understand functional and structural brain connectivity in individuals diagnosed with ASD [9]. The authors show that a disturbance in DMN connectivity might affect social and cognitive symptoms in ASD. In this paper, fMRI data from Autism Brain Imaging Data Exchange (ABIDE) I dataset have been used. The authors used Recurrent Neural Networks (RNN) with Long Short-Term Memory (LSTM) for classifying individuals with and without ASD from the resting-state fMRI time-series, where they achieve an accuracy of 68.5%. The biggest challenge, of the study was achieving a comeptitive accuracy and identifying the critical both spatial and temporal information of the data.

Milan N. Parikh et al. (2019) present a study focusing on the predictive power of Personal Characteristic Data (PCD) from a well-structured dataset from Autism Brain Imaging Data Exchange (ABIDE) database [17]. The study uses six personal characteristics from 851 subjects. The authors use nine supervised machine learning models such as linear and nonlinear SVM, Decision Tree, Logistic Regression, k-Nearest neighbor, Stacked Sparse Auto-encoder (SSAE)-based neural network. Among all the supervised models, the SSAE-based neural network provided the best accuracy of 62%, followed by the k-NN model with weaker sensitivity than the neural network. The authors' biggest challenge was using PCD alone to detect ASD, making the model to identify robust structural and functional complexity of ASD.

Imane Chkifa et al. (2024) aims to develop an early diagnostic system for ASD using resting-state functional MRI (rs-fMRI) data using the ABIDE I dataset in their study [42]. They have used 1,112 subjects that include 539 individuals with ASD and 573 with neurotypical controls aging from 7 to 64 years of the dataset. In their study, CC200, AAL and HO atlases were used with Recursive Feature Elimination (RFE), Lasso regularization and Information Gain analysis as feature selection methods. The study uses Logistic Regression as the classification model for their research and this RFE model and the CC200 atlas achieves 99.66% average accuracy during 10-fold cross-validation. In the context of their study, RFE plays a superior role in feature selection in comparison with the other two methods. The biggest contribution of the author of this study is achieving high cross-validation accuracy on the ABIDE I dataset. The biggest challenge for the study is the use of logistic regression as it does not show major significance like deep learning models for identifying non-linear patterns in the data. Besides, the high accuracy of the study only comes from the cross-validation.

Min Feng and Juncai Xu (2023) develop a robust and unbiased framework for ASD detection in their study. In their study, for analyzing resting-state functional MRI (rs-fMRI) data, they leverage on a custom-designed Convolutional Neural Network (CNN) architecture. They use the specific New York University subset with the age range of 6 to 18 from the ABIDE I dataset. This subset consists of 126 participants, where 56 of them are individuals with ASD and 70 with neurotypical controls. The study uses the Connectrome Computation System (CCS) and the features extraction process also includes motion correction, slice-timing correction, nuisance signal removal and voxel intensity normalization. In the study, the authors use 2D slicing techniques [34]. The slicing process across coronal, sagittal and axial planes provides 22,176 samples for training and testing their model. They capture low-level to high-level spatial features for hierarchical feature extraction by three convolutional layers. For optimizing their model architecture, they use Adam optimizer with a cross-entropy loss function and train 50 epochs with a batch size of 64, achieving 99.39% test accuracy. Since there is a research gap in ASD detection for specifically children and adolescents age group, the authors made their contribution with their model using CNN architecture to minimize the gap. The major limitation of the study is the model not capturing the whole heterogeneity of ASD symptoms.

Lizhen Shao et al. (2023) explore the use of fMRI data and deep learning techniques to detect ASD in children. The authors propose a Heterogenous Graph Convolutional Attention Network (HCAN) model to classify using GCN to detect ASD [38]. Their used model consists of a multilayer HCAN feature extractor and a multilayer perceptron (MLP) classifier. The authors use 871 subjects from the ABIDE I dataset, where 403 participants had ASD and 468 with controls. The model proposed in the paper aims to extract features from a heterogeneous graph by integrating semantic information of different meta-paths with attention mechanisms [38]. The proposed model achieves an accuracy of classification of 82.9%. One of the major limitations of the paper is that the GCN used in the model can only be applied to data with graphs of a specific structure and added subjects would need reconstruction of the graph, resulting in high computational cost.

Ning Qiang et al. (2023) aims to understand brain functional activities by using deep learning models, specially a Hierarchical Recurrent Variational Auto-encoder (HRVAE) [36]. They use HRVAE an unsupervised learning model for fMRI data from ABIDE I dataset, where the encoder of HRVAE's encoder extracts hierarchical temporal features via three hidden layers as a hierarchical feature extractor. The authors use LASSO regression to estimate the corresponding hierarchical functional brain networks. The subject size for their research is 871. The study reports a classification accuracy of 82.1%. The authors make their contribution by using the HRVAE model to discover hierarchical functional brain networks from the fMRI data, potentially enhancing the comprehension of brain disorders like ASD. Additionally, the study also indicates the link between the interactions of hierarchical functional brain networks with brain disorders. The limitation of the study is that the authors don't explore the classification of ASD to enhance ASD detection.

Ali Yousefian et al. (2023) investigates whether graph representation learning methods can appropriately extract the connectivity patterns or not. Among various graph representation techniques, they use AWE, Node2vec, Struct2vec, multi node2vec

and Graph2Img. These embeddings were fed into a LeNet Convolutional Neural Network (CNN) classifier. The study uses 871 individuals from ABIDE I and 910 individuals from ABIDE II, therefore a total 1781 subjects. The fMRI data of these subjects were decomposed into 39 ROIs based on the Montreal Neurological Institute (MNI). The authors achieved notable improvements in ASD classification by using the Graph2Img embedding and LeNet CNN model on the fMRI data. With their research, they achieve 80% accuracy in a rigorous cross-validation setting. There study shows that the usage of embedding vectors is an effective idea, however, this still needs more investigation to find the more suitable graph representation method [40].

Jin Zhang and Fan Feng et al. (2022) address the challenge of ASD detection and emphasises on the potential of neuroimaging data for enhancing diagnostic accuracy, while also acknowledging the constraints posted by the costs and time associated with neuroimaging [41]. The study presents a deep learning approach that combines F-score feature selection technique to improve ASD detection using fMRI data from ABIDE dataset. Their approach validates the network topology for selected features. This approach focuses on metrics like path length and clustering coefficient for analyzing brain network architecture. Their chosen method of F-score is used for feature selection, where the features are analyzed to find these have diagnostic relevance or not and the role these play for characterizing altered brain networks in ASD. The authors achieve an average accuracy of 64.53% on intrasite datasets and 70.9% on the entire ABIDE dataset. The novelty of the study lies in their attempt to combine deep learning with the F-score feature selection method. The authors' limitation is held by the moderate 64.53% inta-site and 70.9% overall accuracy.

A. S. Heinsfield, Alexandre Rosa Franco et al. (2018) aims to apply deep learning algorithms to identify ASD based on their brain activation patterns. They use the resting state fMRI (rs-fMRI) data from ABIDE I repository. The authors include data from 505 individuals diagnosed with ASD and 530 individuals with neurotypical controls. They use functional connectivity to measure correlation between different brain regions. They use network matrices such as degree centrality and eigenvector centrality, while using time-series analysis to capture dynamic changes in brain activity. The study approaches Convolutional Neural Networks (CNNs) for feature extraction from the fMRI data. The study also uses Recurrent Neural Networks (RNNs) to capture temporal dependencies in the data and fully connected layers are employed for classification tasks [13]. Using a combination of supervised and unsupervised learning techniques, the study uses cross-validation to ensure the model's robustness. The authors achieve 70% accuracy in identifying between ASD and control patients. While the authors contribute to ASD detection, their approach and accuracy remain moderate.

Xin Yang, Paul T. Schrader et al. (2020) aim to classify ASD patients with typically developing individuals using functional connectivity features of resting-state fMRI data. The authors use Deep Neural Network (DNN) models on the fMRI data retrieved from ABIDE repository. The study uses the TensorFlow framework to design and implement DNN models. The preprocessing steps of this study include motion correction, normalization and extracting connectivity matrices. For prepro-

cessing they trial 4 techniques, however, the Configurable Pipeline for the Analysis of Connectromes (CPASC) provided the best outcomes [23]. Besides, they use DNN (128-64), which has a configuration of two hidden layers (128 neurons in the first layer and 64 in the second), implying the accuracy of 75.27%. The authors' preprocessing techniques and CPAC's utility provide insightful contributions in ASD detection. However, the reliance on a particular preprocessing technique can also limit applicability.

Thomas Martial Epalle, Yuqing Song et al. (2021) proposes a multi-input Deep Neural Network (DNN) model to amplify the classification accuracy of ASD. With the model they aim to incorporate neuroimaging data processing using three different brain parcellation strategies, reducing dependencies on a single reference atlas. The authors train the model using hinge loss function, eliminating misclassification more strongly. For validating the performance of the model, they employ cross-validation techniques. The study uses 1.038 subjects from the ABIDE I dataset, where they generate 10,038 samples to improve the robustness of the model. The authors achieve 78.07% classification accuracy on the actual data. The novelty of this work lay in their use of a multi-input DNN model with data from three distinct brain parcellation strategies. Although the authors use multiple parcellation strategies, the dependency on these atlases may not address variability in connectivity estimation [27].

Benabdallah FZ, Drissi El Maliani et al. (2023) aim to leverage their theories of under-connectivity and over-connectivity deficits in the autistic brain, ensuring early diagnosis of ASD. The study uses Convolutional Neural Networks (CNNs) and proposes a novel framework enhancing relevant connectivity patterns in brain networks. The authors construct image-like connectivity matrices from functional brain data. They use 871 resting-state fMRI (rs-fMRI) data from ABIDE I repository, employing AAL, DosenBach and CC200 atlases. To identify the patterns distinguishing ASD from neurotypical controls and analyze the enhanced connectivity matrices, CNNs were chosen to be employed. The authors derive image-like connectivity matrices from functional connectivity features of the brain and deploy them as the primary input for the CNN model. The study achieves 96% as cross-validation accuracy. This study contributes in enhancing connections associated with connectivity alterations to improve model performance [32]. This study also provides a unique way to use CNN for neuroimaging tasks, which enables effective pattern recognition.

Yang X, Islam MS, Khaled AA (2019) aims to apply machine learning algorithms to classify individuals with ASD and neurotypical controls using resting-state fMRI (rs-fMRI) data from ABIDE dataset. They deploy their research on a total 1035 subjects, where 505 subjects are of individuals with ASD and 530 with controls. For preprocessing, the authors use C-PAC pipeline that includes slice-time, correction, motion correction and band-pass filtering. The study employs Deep Neural Networks (DNN) and for feature extraction, brain parcellations are applied using 7 different atlases such as- CC400, CC200, AAL, HOA, TT, EZ, Dosenbach, dividing the brain into ROIs. The authors use Pearson correlations between each pair of ROIs to measure functional connectivity. Among all the atlases, CC400 atlas provided the best classification performance, dividing the brain into 400 ROIs. The study uses Logistic Regression, Ridge Regression, Linear Support Vector Machine (SVM) and

Radial Basis Function (RBF), where the Ridge Regression classifier with the CC400 atlas archives the highest accuracy of 71.98%. Although the approach that the authors use holds the advantage of requiring less computational power than the deep learning models, the accuracy they achieve is comparable [19].

Almuqhim F, Saeed F (2021) aim to develop a deep-learning model named ASD-SAENet to classify patients with ASD from individuals with neurotypical controls by using fMRI data from ABIDE dataset. The study uses Sparse Autoencoder (SAE) for dimensionality reduction and feature selection, reducing features from 9.950 to 4,975 in its bottleneck layer. ASD-SAENet efficiently combines a sparse autoencoder for feature selection with a Deep Neural Network (DNN) for classification. The authors extract the features via time series extraction and PCC. The process is evaluated by Peasrson's correlations of 200 regions of the brain. The final classification of the model was based on the softmax layer, outputting the probability of each class. The approach in the study allows the model to capture relevant connectivity patterns associated with ASD from fMRI data, which proves a potentially powerful tool for ASD diagnosis [25].

Sabegh AM, Samadzadehaghdam N et al. (2023) investigates deep learning models such as0 CNNs, LSTMs and hybrid architecture to diagnose autism spectrum disorder (ASD) for resting-state fMRI data from ABIDE I dataset [37]. The authors use 1112 subjects, where 539 individuals are diagnosed with ASD and 573 are of neurotypical controls. They opt for using AAL, HO and CC200 atlas. Most prominent features of the correlation matrix are identified by using the chi-square feature selection method. The architecture they use for their model is Convolutional Neural Networks (CNNs), where they use 2D convolutional layers. For evaluating the process they use a confusion matrix on three statistical criteria such as- accuracy, sensitivity and specificity. The authors use a 10-fold cross-validation technique and achieve 73.53% accuracy for their model.

Bayram MA, Ilyas O et al. (2021) aim to detect ASD using resting-state fMRI data. For the fMRI data, they use the ABIDE I repository. For this paper, the authors use 871 samples, where 403 are of individuals with ASD and 468 with controls. The authors use BASC atlas and calculate the brain network connections through Pearson Correlation Coefficient (PCC) [26]. The authors also convert the 4D fMRI data to functional connectivity matrices, representing temporal and spatial patterns. The study employs CNN, RNN, LSTM and hybrid models such as- CNN with RNN and CNN with LSTM. The CNN layers in the work captures spatial dependencies, while RNN-based models, particularly LSTM captures temporal dependencies of the fMRI data. The best performance of the authors' approach comes from RNN model, where it achieves 74.74% accuracy, following the 74.51% accuracy by BiRNN and 74.4% accuracy by LSTM with 10 fold cross-validation. The best performing RNN includes the model's effectiveness in capturing temporal dependencies in fMRI data for ASD diagnosis.

Ahammed MS, Niu S, Ahmed MR et al (2021) proposes a custom DarkASDNet model in order to detect ASD. DarkASDNet is a Deep Neural Network (DNN) designed to classify ASD from fMRI data by identifying brain connectivity patterns [24]. The proposed model establishes strong diagnostic accuracy, which showcases

the potential of deep learning in neuroimaging for ASD diagnosis. The study only uses the NYU data from the entire ABIDE dataset. The authors use DarkASDNet, inspired by the DarkNet-19 model, which includes 20 convolutional and 6 max-pooling layers. This model efficiently extracts spatial features from the fMRI data slices from classification [24]. The proposed model achieves 94.7% cross-validation accuracy. Although the performance of the model shows potentiality, it is only able to extract the spatial features effectively.

Chapter 3

Background Study

3.1 LSTM: Long Short-Term Memory

Long Short-Term Memory (LSTM) is a particular type of Recurrent Neural Network (RNN), which is designed to solve the problem of learning over long-term dependencies of sequentially chained information.This proposed architecture was for comprising memory cells and gates that control the flow of information. Besides, LSTM layers preserve information on the timeline using memory cells; thus, they are quite effective for time-series data or any sequential data. This also performs well on fMRI data, where the certain patterns of brain connectivity unfold over time. This temporal dependency can be used by an LSTM model for accurately classifying ASD, looking at changes in functional connectivity. This architecture specially deal with both Long Term Memory (LTM) and Short Term Memory (STM) and the set of decisions carried out by the forget, input or learn gate, rememeber gate and use or output gates for making the calculations simple effective as asserted in Figure 3.1 [22].

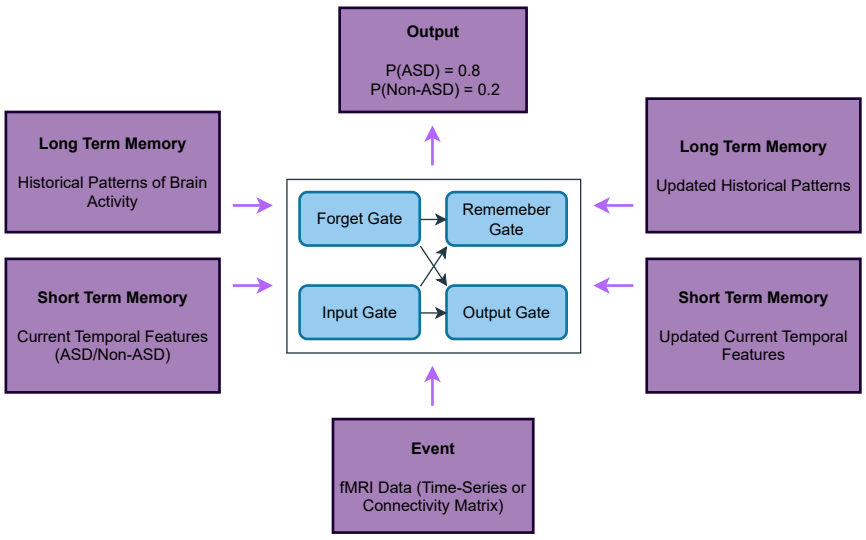

Figure 3.1: LSTM Architecture: Integration of Gates with Long-Term and Short-Term Memory

In training, the network learns these gating mechanisms by means of back propagation. This special ability of control over the flow of information helps it outperform

on sequence-based tasks where dependencies between distant data points that need to be captured. Thus it is considered as one of the state-of-the-art models to work on tasks like time-series forecasting, machine translation, and speech recognition. Together with LSTMs are among the most powerful tools for sequence-based learning tasks, as it can keep track of and process long-term dependencies in data. Identically with their fully component wise memory cell, gate, and flexible architecture, they can accommodate a wide range of applications, from language models up to time-series prediction[22].

LSTM Model Architecture

Forget Gate:

In the LSTM model, the forget gate decides the amount of the cell state that should be retained or dropped based on the input provided. To determine this, the forget gate $f(t)$ is crucial for deciding which information should be discarded or retained from the previous memory state. At each time step t, the forget gate takes the input $x(t)$ and the hidden state from the previous step $h(t-1)$, and applies a sigmoid activation function. The output is a value between 0 and 1, where 0 means "forget everything" and 1 means "keep everything."

$$f(t) = \sigma(W_f x(t) + U_f h(t-1) + b_f)$$

The forget gate activation $f(t)$ is calculated using a sigmoid function σ. Here, W_f is the weight matrix for the input, U_f is the weight matrix for the hidden state, b_f is a bias term, and σ is the sigmoid activation function.

Input Gate:

The input layer of the model normally takes a time-series sequence as input, where each time step contains features extracted from 4D fMRI data regarding the functional connectivity of the brain over time. Here, preprocessed data from the ABIDE I dataset is fed as input vectors to the network at every time step. The inputs are sequences of 3D fMRI images which describe the brain activity over time. For any given sequence, each one of those time steps corresponds to a volume of brain activity—a 4D dataset, including x, y, z, and time. It is possible to reshape the input data into a two-dimensional array where each row represents a time step in the fMRI sequence.

The input gate $i(t)$ controls what new information should be added to the cell state. It ensures that the cell state is updated with relevant new data from the current input and the hidden state. The gate applies a sigmoid activation to the input and hidden state, while the candidate cell state is calculated with a tanh activation function.

$$i(t) = \sigma(W_i x(t) + U_i h(t-1) + b_i)$$
$$\tilde{C}(t) = \tanh(W_c x(t) + U_c h(t-1) + b_c)$$

The input gate activation $i(t)$ is calculated using a sigmoid function σ, where W_i defines the weight matrix for the input, U_i defines the weight matrix for the hidden state, and b_i is the bias term. To calculate $\tilde{C}(t)$, the tanh activation function is used, and W_c and U_c are the weight matrices for the candidate cell state. The input

gate determines how much of the current input should be added to the cell state. It works together with the candidate state $\tilde{C}(t)$, which is the proposed new content to be added to the memory. The result of the sigmoid function varies between 0 and 1, controlling how much of this new candidate state is incorporated into the memory.

Cell State Update:

After both the forget and input gates have made a decision about what to throw away and add, respectively, the cell state is updated. The memory cell $C(t)$, also known as the cell state, stores information over time. It is updated by the combined effects of the forget and input gates. The forget gate determines how much of the previous cell state $C(t-1)$ to keep, and the input gate controls what new information is added.

$$C(t) = f(t) \odot C(t-1) + i(t) \odot \tilde{C}(t)$$

The cell state $C(t)$ is updated by combining the new candidate values, where $f(t)$ denotes the forget gate output, $i(t)$ denotes the input gate output, $\tilde{C}(t)$ specifies the candidate cell state, and $\odot$ denotes element-wise multiplication. The memory cell combines the retained information from the forget gate and the new information from the input gate, enabling the Long Short-Term Memory Networks (LSTM) to preserve useful long-term information and get updated with relevant new data.

Output Gate:

The output gate calculates the hidden state, which is used for predictions and passed to the next time step. Here, $o(t)$ determines what part of the current cell state should be output as the hidden state $h(t)$, which will be passed to the next time step. The gate applies a sigmoid function to the current input $x(t)$ and the previous hidden state $h(t-1)$, and the output is modulated by the tanh of the cell state.

$$o(t) = \sigma(W_o x(t) + U_o h(t-1) + b_o)$$

$$h(t) = o(t) \odot \tanh(C(t))$$

The output gate activation $o(t)$ is calculated using a sigmoid function σ. Here, W_o denotes the weight matrix for the input, U_o defines the weight matrix for the hidden state, and b_o is the bias term. The output gate determines what the Long Short-Term Memory Networks (LSTM) block will output at the current time step. It controls which information from the current cell state $C(t)$ should be passed to the next step. This output becomes both the final output of the Long Short-Term Memory Networks (LSTM) at this time step and the hidden state $h(t)$ for the next time step[43]. At each time step, the LSTM block updates its cell state based on inputs from the forget gate and the input gate, while the output gate determines the block's output. It has the ability to remember long-term dependencies as well as discard the information that is irrelevant. Equally these gates enable the LSTM to mitigate the vanishing gradient problem by ensuring the information relevant to long sequences is retained. coupled with forgetting the unnecessary information. Thus it can perform as the most highly effective for task management such as time series prediction, language modeling, and sequential data analysis.

3.2 GRU: Gated Recurrent Unit

Gated Recurrent Unit (GRU) is a type of Recurrent Neural Network (RNN), introduced by Cho et al. (2014) [4] as a simpler alternative to Long Short-Term Memory (LSTM) networks that can process sequential data such as text, speech and time-series data. Similarly to the LSTM unit, the GRU has gating units that modulate the flow of information inside the unit, but without having separate memory cells [5]. GRU combines the forget and input gates and parameters which simplifies the model, making it computationally more efficient than LSTM while still addressing the vanishing gradient issue. This advantage makes GRU fitting for tasks when training needs to be faster or where provided with limited computational resources [44]. Moreover, GRU is also well-suited in several applications because of its ability to capture long-term dependencies with fewer parameters, making it a desirable alternative to LSTM at many uses [33]. The efficiency of GRU lies in its architecture containing two gates: the update gate u_t and the reset gate r_t and a candidate hidden state $\tilde{h}_t$.

GRU Model Architecture

Update Gate:
The update gate determines which information is necessary to carry forward to the current time step. The update gate is denoted by z_t that is calculated using the current input x_t and previous hidden state h_{t-1} where σ (sigmoid function) gives output between 0 and 1, z_t value determines the balance between h_{t-1} and $\tilde{h}_t$. If the value of z_t is close to 0, the model relies more on the new candidate state and for 1, it relies more on the previous hidden state. The model combines the previous hidden state ht-1 and candidate state h t, weighted by update gate u_t, to get the final hidden state h_t [8].

$$z_t = \sigma(W_z x_t + U_z h(t-1))$$
$$h_t = z_t \cdot h(t-1) + (1 - z_t) \cdot h_t$$

Reset Gate:
The reset gate, denoted by r_t, determines how much of the previous information to forget while calculating the new candidate hidden state. The rest gate r_t uses current input x_t and previous hidden state h_{t-1}, σ (sigmoid function) limits r_t between 0 and 1 [8].

$$r_t = \sigma(W_r x_t + U_r h(t-1))$$

Here, r_t decides how much of h_{t-1} affects the candidate hidden state $\tilde{h}_t$. While r_t is close to 1, the previous hidden state determines the new candidate, and its closing at 0 indicates that the unit's memory is resetting, minimizing the influence of the previous hidden state.

$$\tilde{h}_t = \tanh(W_h x_t + U_h(r_t \cdot h_{t-1})$$

Moreover, the candidate hidden state represents the new content to be added to the current hidden state regulated through the reset gate [8]. The rest gate allows GRU to ignore irrelevant past information with a selective approach, making it more efficient to capture short-term dependencies [30].

3.3 CNN: Convolutional Neural Networks

Convolutional Neural Networks (CNN) is one kind of deep learning model that can process grid-like data, especially image data. The architecture of this model effectively captures the spatial and temporal dependencies in the data through several layers of the model and hence it is very efficient for image data [31]. Applications of CNN are many, including image classification, image semantic segmentation, object detection in images, etc., where several specialized and unified layers process and analyze the given data[10]. CNN is structured as a series of stages. The first few stages are composed of two types of layers: convolutional layers and pooling layers such that between each convolutional layer there is pooling layer.

Input Layer:

In the context of image data, this most often involves the intake of pixel intensities, represented as a multi-dimensional array to capture the spatial and color dimensions of the visual information[2].

Convolutional Layer:

Units in a convolutional layer are organized in feature maps. Within this, each unit is connected to local patches in the feature maps of the previous layer through a set of weights named filter banks. The gained outcomes of this local weighted sum is then passed through a non-linearity like ReLU. The same filter bank is shared among all units, but different feature maps in a layer use different filter banks [6]. This layer adds a set of filters or kernels to the input image that screens for identifying features such as texture, color or edges in the picture. Moving over the input, each filter then computes a dot product with overlapping regions that generates a feature map [31]. In the equation below, I stands for input image, filter is K and output featured map is F at i, j position.

$$F(i,j) = (I * K)(i,j) = \sum_m \sum_n I(i+m, j+n) \cdot K(m,n)$$

Activation Layer (ReLU):

The Rectified Linear Unit (ReLU) activation function provides non-linearity to CNN so that it can go through complex patterns. In the feature map, the ReLU function is applied as-

$$f(x) = max(0, x)$$

In this equation, the input value is x. ReLU keeps only the positive values that help in reducing computational complexity [7].

Pooling Layer:

Even Though the convolutional layer detects local conjunctions of features from previous layers, the role of the pooling layer is to merge features that are semantically similar. A pooling unit computes the maximum of a local patch unit in a feature map. In this layer, the spatial dimensions of the feature maps are reduced that reduces computational complexity as well. The commonly used pooling technique is max pooling, which takes the maximum value in each subregion of the feature map.

In the equation for the max-pooling operation below, F defines the feature map, (m, n) are the specifications of the pooling region, and P(i,j) is the output.

$$P(i, j) = \max\{F(i + m, j + n)\}$$

Fully Connected Layer:

All the previously extracted features are combined at a fully connected (FC) layer in order to make a final classification. Every neuron of the FC layer connects with every neuron in the previous layer. In the output equation below, W portrays the weights, x is the flattened input vector from feature maps, b stands for bias and f is an activation function.

$$y = f(W \cdot x + b)$$

Convolutional Neural Networks are able to provide a powerful yet efficient way of analyzing data presented in grid-like format, especially images, by catching the spatial and temporal dependencies based on a series of convolution and pooling layers. The hierarchical feature extraction at different levels makes CNNs ideality suitable for tasks regarding image classification and object detection. Functional connectivity matrices, which express the strengths of interaction between different parts of the brain, have indeed been one of those places where CNNs have captured spatial patterns effectively, important for ASD classification.

Chapter 4

Methodology

4.1 Dataset Description

For this research we mainly focus on the Autism Brain Imaging Data Exchange (ABIDE I) preprocessed dataset which is a large-scale neuro-imaging database of individuals of the Autism Spectrum Disorder (ASD) and neuro-typical individuals. This large-scale database integrated the neuroimaging and phenotypic data from subjects with ASD diagnoses and typically developing controls.Nilearn, a Python-based neuroimaging toolkit `datasets.fetch_abide_pcp()` assist in fetching the ABIDE data by connecting directly to the dataset repository on the S3 server. Our reserch has set parameters such as the number of subjects, pre-processing pipelines, and filtering options in accordance with our specifications to download only the relevant subset of data. Once the data is fetched, preprocessing steps are applied to make it suitable for analysis. The raw spatio temporal fMRI data, which represents brain activity over time, is reduced to a 3D representation by calculating the mean image across all time points. For better interpretability, non-significant brain activity is thresholded out so that only a clear visualization of regions with significant function remains. This not only reduces the noise but also brings into view a pattern of brain connectivity pertinent to ASD. The ABIDE I dataset was contributed by 18 different sites including elite institutions like the University of Pittsburgh School of Medicine and the University of California, Los Angeles , etc with a total of 1,112 subjects. Among these, 539 individuals are diagnosed with ASD, while 573 are typically developing controls, providing a balanced dataset for comparative studies.

Furthermore, ABIDE includes extensive demographic details or phenotypic file such as age, gender, IQ scores (verbal, performance, and full-scale), and handedness, as well as detailed scanning parameters including scanner type, repetition time, echo time, flip angle, and the duration of fMRI experiments. Some of which has been depicted in Figure 4.1 which is a correlation heatmap of various phenotypic features, including age, Full IQ (FIQ), Verbal IQ (VIQ), and Performance IQ (PIQ). It depicts the strength and direction of correlations between these attributes using color intensity.

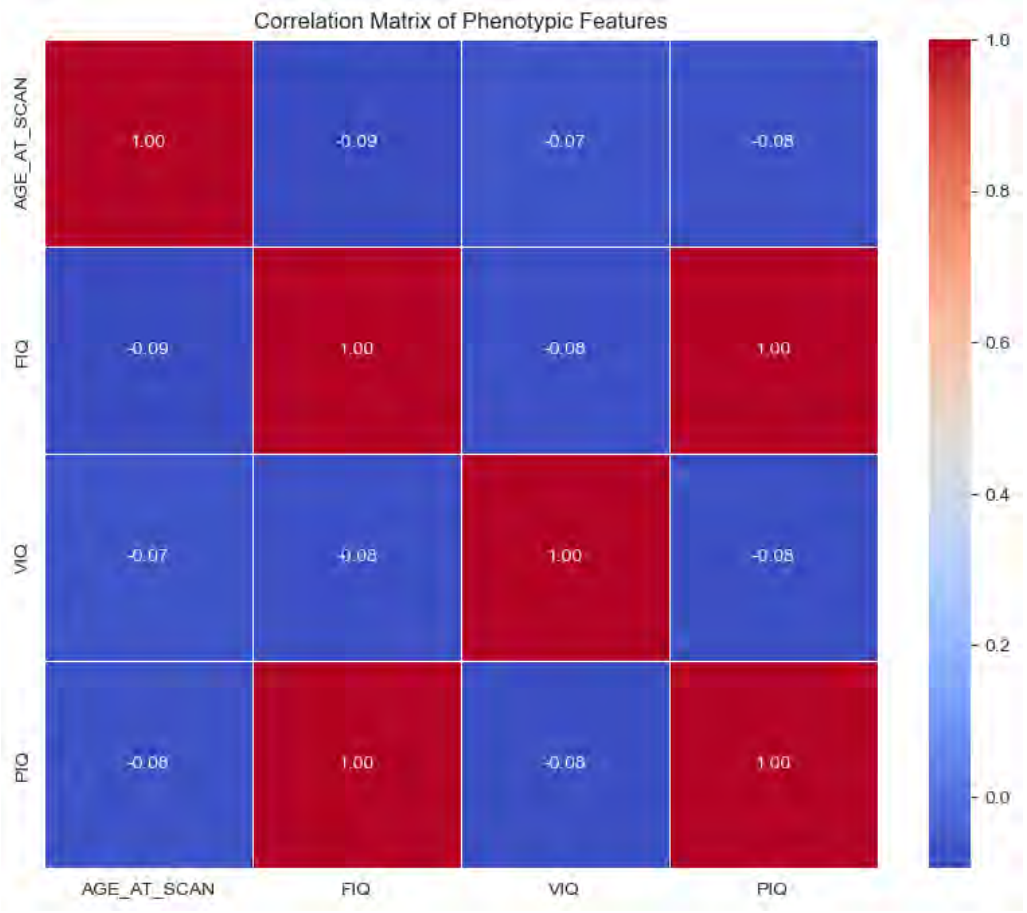

Figure 4.1: Displaying the 4D Brain Slice

Age Stratification Across ASD and Control

The age range of participants in this dataset is from 7 to 64 years[21]. Thus allow detailed investigations across the different developmental stages-from childhood through adolescence into adulthood. These are further divided into three main groups based on this wide age range: Children: from 2 to 12, Adolescents: from 13 to 18 and Adults: from 19 to 64. This stratification enable this research to study how the patterns of brain connectivity evolve across different life stages in individuals with ASD, offering critical insights into the developmental trajectory of the disorder. The study is confined to participants within the age range of 2 to 18 years, as defined by the parameter AGE_AT_SCAN = (2.0, 18). This age range allows us to focus on developmental stages most relevant to the investigation of Autism Spectrum Disorder (ASD). Within this cohort, a total of 334 individuals are classified as neurotypical controls, while 285 individuals are diagnosed with ASD. The distribution of participants across these diagnostic groups was retrieved using the DX_GROUP field from the abide.phenotypic dataset, offering a clear distinction between the control and ASD groups for further analysis.
The bar chart of Figure 4.11 display the distribution of the subjects into two diagnostic categories, namely ASD and Control. Specifically, this chart demonstrates a fair distribution of participants between the two groups between the mentiones age. The graph mainly shows that both the ASD and Control groups are represented by almost identical counts. Complementing this, the histogram of Figure 4.2

focus on the granular look at the age distribution within each diagnostic group via a histogram. Here the blue curve,represent the ASD group, and the orange one, represent the Control group, provide a representation of the age characteristics of these populations. It also depict that most of the subjects are within a common developmental range, which is important in interpreting the temporal dynamics of brain development and neural activity in both ASD and Control groups. The bar chart in Figure 4.2 ensures that the dataset is well-represented across the mentioned two groups, which is an unbiased analysis and comparison. On the other hand, the histogram in Figure 4.11 focuses on the age-dependent factors that might influence neural development and behavioral characteristics, especially in the context of ASD. From these distributions, we can tell if the sample is representative or not and investigate potential age-related biases affecting the modeling or analysis of ASD.

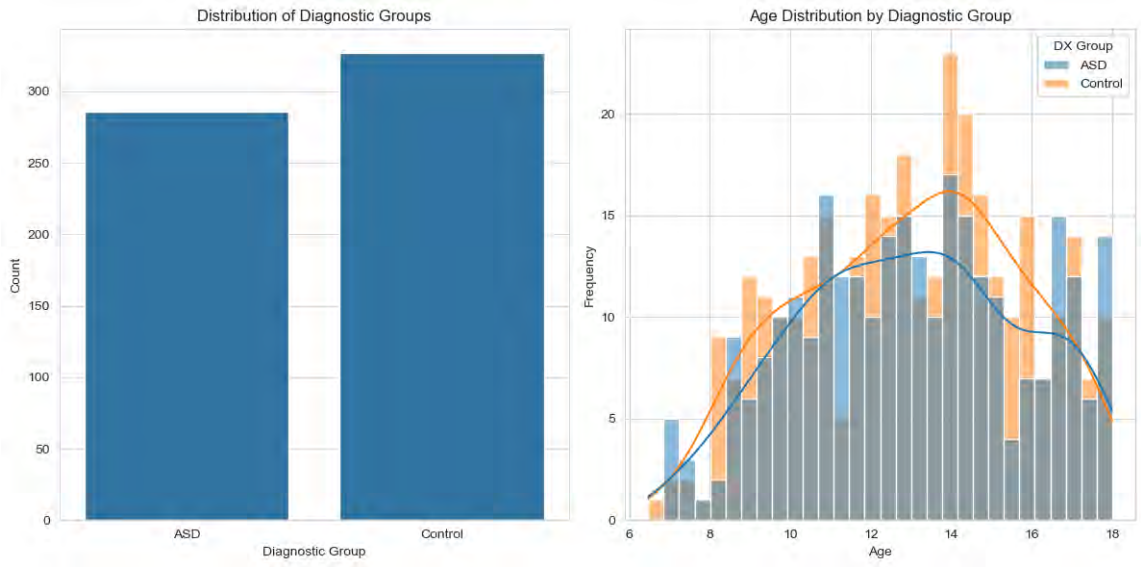

Figure 4.2: Diagnostic Group Distribution and Age Stratification Across ASD and Controls (Aged 2-18)

4.1.1 Effectiveness of 4D Dataset:

This functional MRI data has been regarded as 4D since it includes three spatial dimensions: x, y, and z, with a temporal dimension, t. It is in this 4D format that the data of fMRI are particularly powerful because it enables the study of dynamic brain activity across time.
In a typical fMRI scan, a volume of the brain at multiple time points is acquired, moving one 3D image at every step in time. The time steps here represent the activation of the brain at different instants during the scan. Which allows us to trace the way various regions of the brain activate in concert with one another. Temporal dimensions in this 4D data, especially in functional connectivity studies, bring out substantially in disclosing the correlations between different brain regions' activation patterns.

- The dimensionality of this dataset can help in tracking the dynamic changes that occur during brain activity and help to identify the temporal communication of different brain areas.

- Spatially, this analysis allows for the investigation of the relations between brain regions for a group of subjects at different time points.

- Brain connectivity is also a temporal process, which can be defined as a temporal evolution. This evolution plays an important role in brain malfunctioning conditions such as autism.

Due to the intrinsically 4D nature of the data, the analysis often becomes really tricky and requires advanced processing techniques to capture meaningful relations between the regions over time.

4.1.2 Dataset Complexity

This dataset is complex both in its size and variability intrinsic to the data. Every fMRI scan consists of thousands of voxels, 3D pixels representing different regions of the brain and the brain has been divided into 116 regions. Given that each voxel has a time series of brain activity recorded over several time stands, the dataset quickly grows massive and multidimensional.

- **Dimensionality:** Each fMRI scan is represented as a 4D dataset, leading to an enormously high number of features (voxels), which results in high-dimensional data that is hard to model.

- **Feature Selection:** All the voxels in the brain are not contributing equally to the functional connectivity pattern. Selecting the most relevant voxels or regions of interest is one of the most indispensable steps toward reducing the level of noise and avoiding overfitting of any machine learning model.

- **Motion Artifacts:** fMRI data usually suffer from motion artifacts, which occur, in particular, in young children. These artifacts add Gaussian-distributed noise to time series data which allows 24 motion parameters to be regressed out during preprocessing.

- **Long-term Dependencies:** Brain activity can depict both short-term and long-term dependencies. In other words, it means interaction between time points far apart has to be modeled, which the standard machine learning models are not designed to handle. Even the LSTM and Bi-LSTM networks share this challenge because of the complexity of the brain signals.

- **Functional Connectivity:** This would include the measurement of functional connectivity by calculating the correlations between different time series emanating from different regions within the brain. Working with the correlation matrices capturing the relationships between hundreds of regions within the brain adds another layer of complexity.

- **Overfitting:**Deep learning models are prone to overfitting due to the high dimensionality of the data and the relatively limited number of subjects. A careful regularization and cross-validation will be in order for generalization on new data.

- **Training Time:**Especially the LSTM and BiLSTM models are quite time-consuming because both these models have to capture temporal dependencies that exist over hundreds of time steps in highly complex data.

- **Matrix Size:** Functional connectivity matrices are usually very large, including many regions of interest. This would imply a single-subject matrix, including several thousand correlation values to be considered.

- **Inter-Subject Variability:**The connectivity matrix stemming from each subject is different, and finding common patterns or differences between ASD and TD subjects requires automatic recourse to sophisticated techniques of clustering or dimensionality reduction.

Even with preprocessed ABIDE data, the complexities are still immense regarding the structure and interpretation of high-dimensional fMRI data. Temporal and spatial characteristics of the data require some sophisticated modeling with LSTM or BiLSTM networks to represent underpinning patterns. Further, variability within subjects, coupled with inherent challenges in interpreting functional connectivity, makes this data inherently difficult to handle from both computational and sophisticated modeling standpoints.

4.2 Spatio-Temporal Data Visualization

This data set is mainly a composition of neuroimaging data, such as resting-state fMRI and sMRI scans. That in turn helps to investigate the structure of the cerebral and its function, particularly emphasizing the functional connectivity of the brain. It is important in the investigation of the spontaneous activity of the brain, independent of external stimulation, which has become a critical modality in the investigation of functional connectivity. Thereby, studies have been able to reveal significant differences in functional connectivity in individuals with ASD from neurotypical controls, particularly within those networks of the brain that form the basis of social behaviors and cognitions. The most significant and valuable element of this dataset is that it is especially based on resting-state fMRI. Resting-state fMRI scans record instances of the spontaneous activity of the brain in rest and thus are of particular help when it comes to investigating functional connectivity, that is, interaction of different brain regions in a state of rest while the person does not perform any particular task. Resting-state fMRI data are fundamental for describing disrupted networks that form the basis of the social and cognitive impairments demonstrated by individuals with ASD. Commonly, studies have indicated that ASD individuals show abnormal connectivity within the brain networks that form the base for social cognition and empathy and in those networks implicated in executive function.

4.2.1 Interactive 3D Mapping of Brain Activity

The visualization of the 4D data's dynamic view can uncover spatial-temporal patterns that is critical to understand. The visualization of a 3D mean image derived from a specific 4D fMRI file in the ABIDE dataset has been depicted in the Figure 4.11. The `abide.func_preproc[100]` is a 4D fMRI file, where the four dimensions represent. The first three dimensions are the spatial coordinates (x, y, z), defining the brain's structure. The fourth dimension is time, representing the fluctuations in brain activity across different time points during the fMRI scan. The function `image.mean_img(img)` calculates the mean image by averaging the signal intensity across all time points for each voxel (3D pixel) in the brain. This results in a 3D image where each voxel reflects the average activity over the entire scan duration. The parameter is set to `threshold=2`, which sets a lower bound, such that only regions with signal intensities above the threshold are visualized. This process mainly removes non-significant or low-activity areas, enhancing the visibility of regions with meaningful brain activity. The `dim=-0.3` parameter adjusts the brightness and contrast of the visualization, emphasizing the structural and functional regions of interest in the brain. The function `plotting.view_img` is used to render an interactive 3D visualization of the mean brain image. This helps to visualize and observe which regions of the brain exhibit significant mean activity. Additionally this also offer a understanding of the overall brain functionality during the brain scanning. This visualization presented in Figure 4.3. serves as a generalized representation of brain activity for the subject corresponding to `func_preproc[100]`. It highlights the regions that has the consistent activity throughout the process if scanning. As well as are useful in identifying regions of interest and serve as input for further analyses, such as computing functional connectivity or training machine learning models.

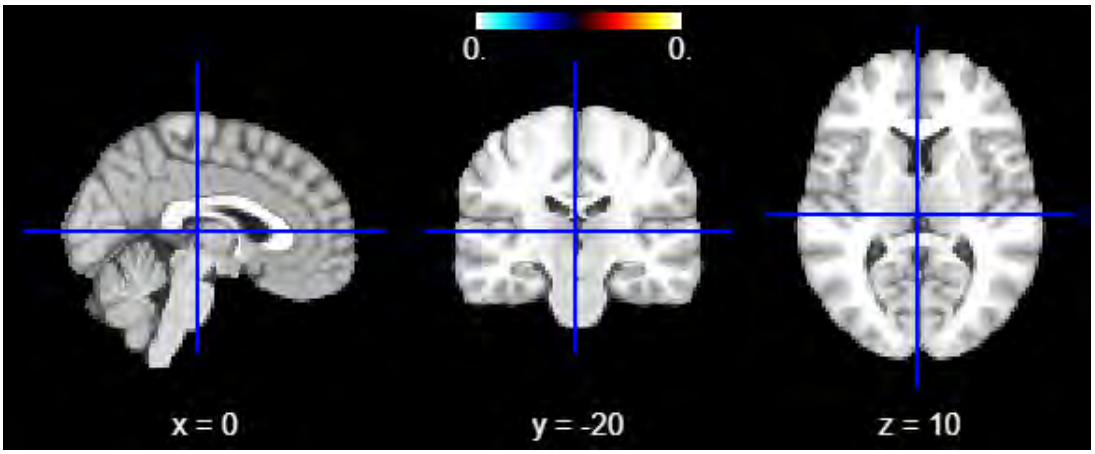

Figure 4.3: Spatiotemporal Dynamics and Visual Mapping of Brain Activity: 3D Mean fMRI Imaging

4.2.2 Glass Brain Visualization

To demonstrate the generation of a glass brain visualization depicted in Figure 4.4, a technique has been used to display the structural and functional attributes of the brain in a transparent, three-dimensional format. First, the mean functional image

from a 4D fMRI dataset needs to be calculated. This reduces the 4D data (spatial and temporal dimensions) to a 3D representation where each voxel reflects the average signal intensity across time points. Then a threshold is set dynamically at 10% of the maximum voxel intensity ($0.1 \times$ max intensity), ensuring only significant regions are highlighted. This approach specially captures the small amount signal changes even, that make it ideal for visualizing low-intensity yet meaningful activity patterns. The `plot_glass_brain` function generates a transparent 3D rendering of the cerebral. Similarly, the `display_mode='ortho'` shows orthogonal views (sagittal, coronal, axial), providing a comprehensive spatial overview as illustrated in Figure 4.4.

By applying the small number of thresholds, the visualization could capture both high-activity regions and subtle, nuanced changes. Since in some cases this are often ignored in standard thresholding approaches. The glass brain overlay the functional data on the transparent anatomical outline that provides a global perspective. Apart from this the thresholding has effectively removed background noise and the areas having low-activity, which helps in emphasizing meaningful brain regions. On the top of that it is useful for identifying global activity patterns associated with neurological disorders as well as aids in exploring brain activity trends without delving into voxel-level details. This glass brain visualization is an elegant tool for inspecting the overall comprehensive and the interpretable brain activity of a individual in a specific time point.

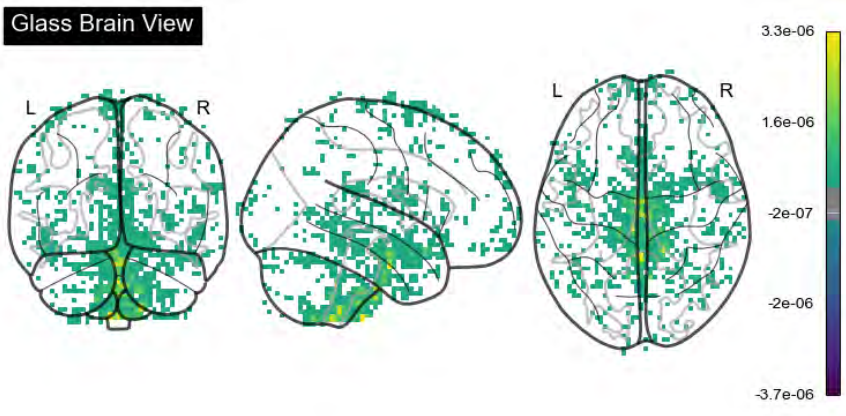

Figure 4.4: Dynamic Glass Brain Visualization: Capturing Subtle Functional Variations

4.2.3 Visualization of Brain Connectivity

The connectome visualization using a randomly generated connectivity matrix and node coordinates highlights the spatial and functional relationships between different regions of the brain in a network graph format that has been demonstrated in Figure 4.5. To visualize that, a 20x20 connectivity matrix is generated, where each element represents the strength of connectivity between two nodes (regions of interest in the brain). Random values are used here for illustration, mimicking a realistic brain connectivity matrix. Further, the coordinates of 20 nodes are randomly generated within a typical brain space range ($[-60, 60]$) in 3D space, representing the anatomical positions of the brain regions. Here, the nodes represent specific brain

regions, and edges depict connections between regions, scaled and colored according to their strengths.
The graphical representation offers an interconnected representation of brain connectivity that is biologically contextualized and helps to visualize how different parts of the brain interact and communicate by adjusting the attention from individual brain regions to interregional interactions. This is essential for analyzing both anatomical and functional connections, including white matter territories and the co-activation patterns during tasks. The thresholding of edges ensures that only the most significant connections are displayed, reducing visual clutter and emphasizing the core network architecture. The connectome is suitable for understanding the complex network of the brain and assists in detecting disrupted connectivity patterns in neurological disorders (e.g., Alzheimer's, autism). Exploring brain network properties like hubs, modularity, and integration.

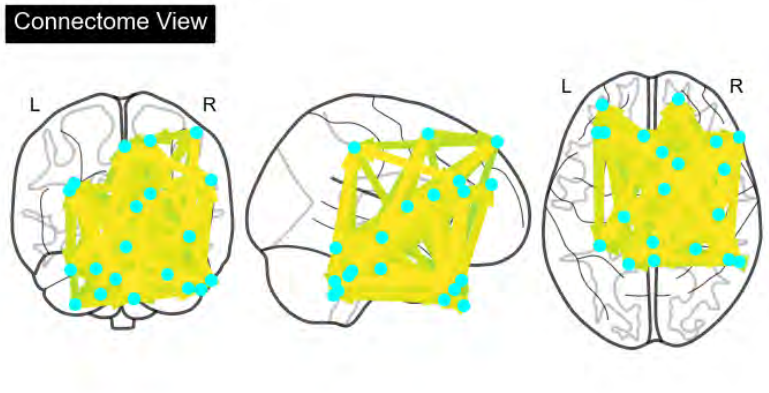

Figure 4.5: Dynamic Visualization of Brain Connectivity: A Connectome Perspective

4.2.4 Orthogonal EPI Visualization

The visualization of a single volumetric slice from a 4D fMRI dataset using Echo-Planar Imaging (EPI) techniques has been depicted in Figure 4.6 and Figure 4.7. The raw 4D fMRI dataset has been directly loaded, where the first three dimensions represent spatial coordinates (x, y, z), and the fourth dimension represents time (temporal dynamics of brain activity). Using the nilearn_image.index_img function, a single 3D volume (first time point) has been extracted from the 4D data for analysis. Following that, the extracted volume is visualized in orthogonal views (sagittal, coronal, and axial). Meanwhile, the data has been displayed with a grayscale colormap for simplicity and standardization in brain imaging as dsplayed in Figure 4.6. This is ideal for preserving data fidelity and ensuring comparability as well. And by utilizing the perceptually uniform 'viridis' colormap, the contrast has been enhanced and subtle variations in intensity made more discernible, which has been potrayed in Figure 4.7. This specially highlights subtle variations in voxel intensity, aiding in the identification of distinct brain structures or artifacts. display_mode='ortho' ensures orthogonal (3-plane) visualization for comprehensive spatial coverage, and the cut_coords=(0, 0, 0) automatically centers the cross-section at the brain's origin, providing a standard reference point.

Extracting and visualizing a single volume allows us to inspect the spatial quality of the data for artifacts, noise, or distortions and helps in examining anatomical features and functional contrasts within a single temporal snapshot. Additionally, it aids in identifying structural or functional abnormalities in specific time points and verifying preprocessed data before advanced analysis like statistical modeling or machine learning. In advance of combining the data for temporal analyses such as task-related activation studies or functional connectivity, this illustration aids in the evaluation of the statistical significance of individual time points.

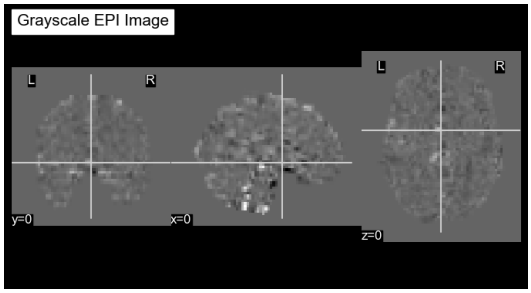

Figure 4.6: Orthogonal EPI Visualization: Grayscale

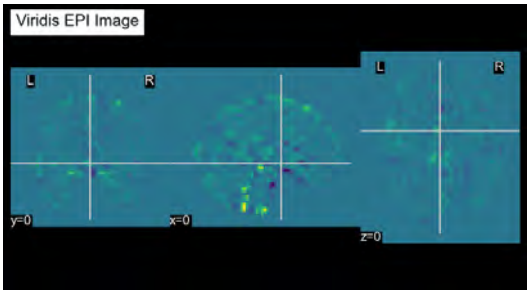

Figure 4.7: Orthogonal EPI Visualization: Enhanced Contrast Renderings

4.2.5 Contrast-Enhanced Smoothed EPI Visualization

The illustration of smoothing of a single volume from a 4D fMRI dataset and visualizing it with adjusted contrast settings has been portrayed in Figure 4.8. To assist the visualization, the smooth_img function applies a Gaussian smoothing kernel with an FWHM of 6 mm. This processes the voxel intensities within a specified radius, effectively reducing noise while preserving underlying patterns. In particular, the smoothing enhances the signal-to-noise ratio (SNR), facilitates better spatial localization by suppressing high-frequency noise, and prepares the data for further statistical analyses or visualization. The smoothed volume is visualized in sagittal, coronal, and axial slices using plot_epi with the following adjustments. This allows us to verify the spatial smoothing process, which helps to reduce artifacts and ensures the dataset is well-prepared for statistical modeling. Apart from this, vmin=100 and vmax=1000 primarily set the intensity range for voxel values, ensuring better contrast and highlighting significant regions. By adjusting contrast, subtle intensity variations that might be obscured in raw data become more discernible. Besides, the resampling_interpolation='nearest' maintains the integrity of voxel data by avoiding overly aggressive interpolation during resampling. Additionally, the volume is labeled as "Sample EPI Image - First Volume," with the cross hairs centered at the origin coordinates $(0, 0, 0)$.
Before moving on to more advanced studies like statistical parametric mapping or machine learning-based categorization, the illustration in Figure 4.8 helps our research to assess the first stage of the pipeline through contrast adjustment and smoothing. As this has examined anatomical and functional brain regions, and bridging the distinction between raw data and analytical readiness.

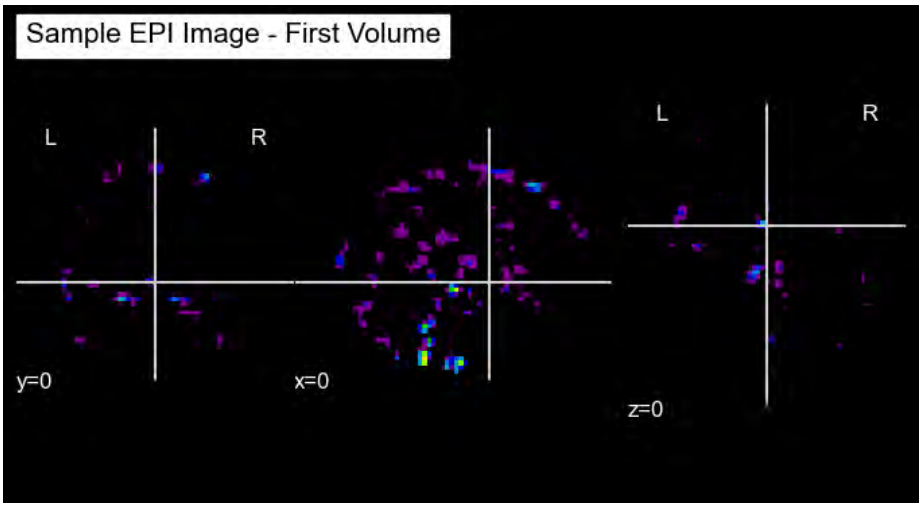

Figure 4.8: Contrast-Enhanced Smoothed EPI Visualization

4.3 Initial Approach

The first framework integrates neuroimaging and machine learning for Autism Spectrum Disorder (ASD) classification using fMRI data. The ABIDE I dataset is preprocessed to reduce dimensionality and filter noise, yielding a clearer representation of brain activity. Firstly the spatiotemporal features are extracted using the AAL, Dosenbach, and Schaefer atlases, segmenting the brain into regions of interest and providing time-series data and functional connectivity matrices.Deep learning models are employed, including LSTMs for temporal dependencies, BiLSTMs for bidirectional insights, GRUs for computational efficiency, CNNs for spatial pattern analysis, and GCNs for graph-based connectivity learning. And by taking the best component from LSTM and GRU an ensemble model has been developed that the combines outputs from LSTM and GRU to maximize performance. Optimization techniques like Adam optimizer, regularization, early stopping, and hyper-parameter tuning ensure robust training. The workflow in Figure 4.9 demonstrated the overall initial approach that delivers a comprehensive, efficient system for ASD classification, leveraging both temporal and spatial brain connectivity features.

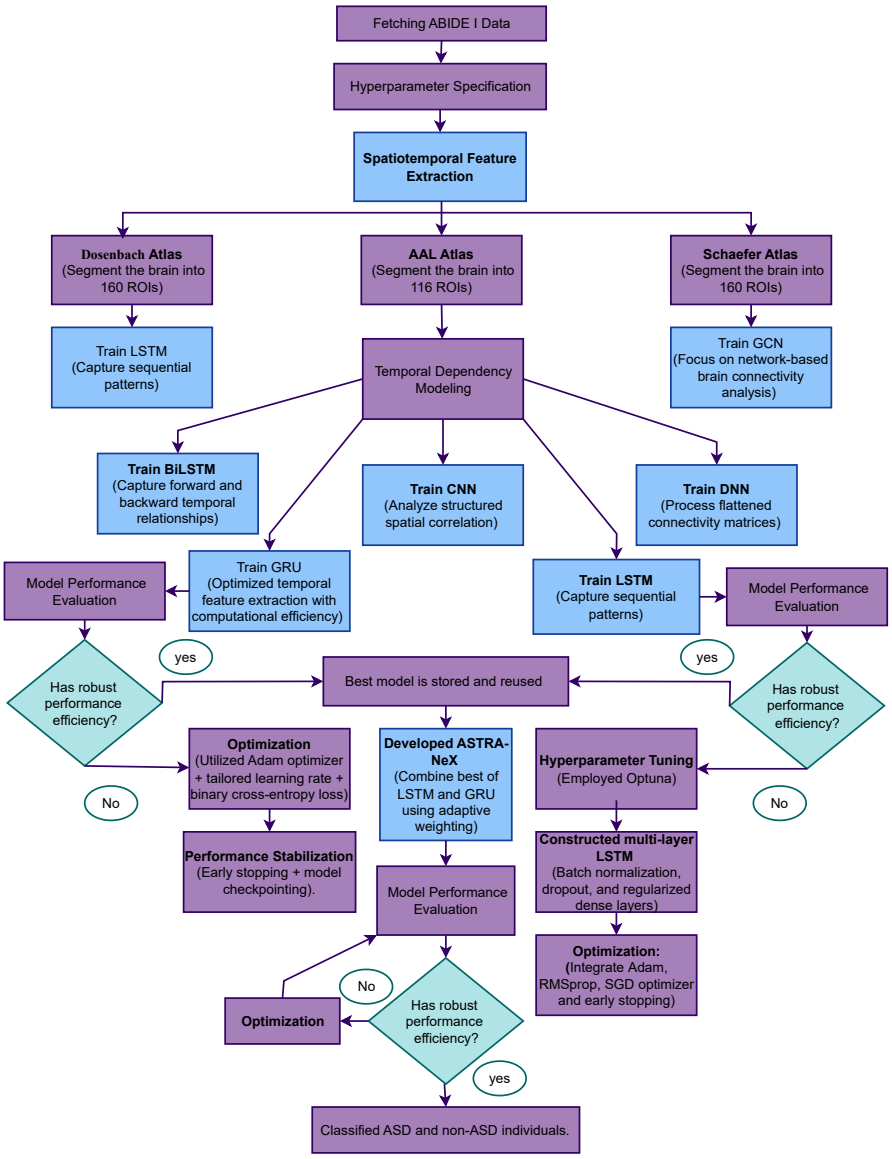

Figure 4.9: Initial Approach

4.3.1 Spatiotemporal Feature Extraction

Atlas Selection and Masker Configuration

AAL Atlas: AAL Atlas has been used to segment the brain into regions of interest (ROIs). This atlas specially divides the brain into 116 regions based on anatomical landmarks. Before extracting the features, we fetched Automated Anatomical Labeling (AAL) atlas using fetchatlasaal(). This atlas provides us a set of predefined regions of interest (ROIs) in the brain, which we used to extract signals from specific areas of the brain. Moreover, NiftiLabelsMasker masker has been configured to process the functional MRI data according to this atlas. With the help of the masker, we can resample the atlas to match the data, detrend the signals to remove linear components, standardize the signals to a mean of zero and standard deviation of one per scan, and remove high variance confounds to minimize noise and artifacts.

Dosenbach Atlas: The application of the Dosenbach atlas within this research

provides an effective method of analysis in the large-scale functional connectivity profile across different regions of the brain. 160 ROIs can be identified using rs-fMRI data, focused on cognitive control, task, and motor control-related networks. This atlas also facilitate the examination of functional connectivity within the human brain at the macroscopic level. For ASD classification, the Dosenbach Atlas aids in studying disrupted functional connectivity patterns across these networks. Which allows for targeted analyses on ASD-specific neural signatures by focusing on regions that are known to be involved in social cognition, executive control, and sensorimotor functions. We implmented this atlas for LSTM model as it is particularly well-suited for Long Short-Term Memory (LSTM) networks, as it provides detailed temporal patterns of connectivity.

Schaefer Atlas: This atlas integrates functional connectivity profiles from large datasets to divide the brain into 400 ROIs or customizable ROIs, such as 100, 200, 300, etc. This flexibility easily enables one to balance computational efficiency against anatomic precision. Particularly thsi is used in network-based analyses as well as for most of the machine learning models that require fine-grained representations of functional connectivity. Fine-grained parcellation of the Schaefer Atlas is extremely suitable for a detailed examination of subtle alterations in patterns of functional connectivity in ASD versus non-ASD subjects. It helps in outlining ASD-specific disruptions of network, specially the social and sensory networks. As Schaefer Atlas particularly apt for GCNs so this research has implement GCN from the extracted features of this atlas. By using this extracting fearutres the connectivity matrix will represent the adjacency matrix of the GCN, allowing the model to learn patterns both locally and globally in the connectivity.

4.3.2 Feature Extraction via Atlas

Time Series Extraction

In the ABIDE I dataset, for each subject, wetransformed the functional MRI data (abide.funcpreproc) using the configured masker. By doing this we can extract and store the time-series data for each region defined in the each atlas for the brains. The time series signals represent activities of the brain in different regions for each subject in a certain time. In the first place temporal developments of the brain activities of an individual are reflected through time series signals. Each time series is a sequence of data collected with time, where the x-axis shows time points, and the y-axis represents signal intensity. Secondly the time series can be plotted of any subject between 0 to 612 to visualize the signal variations across different time points for the 116 brain regions. In the Figure 4.11 each "time point" is the time it takes to scan the whole brain of an individuals once, taking the signal from many parcellations of the brain. Thus, for a participant, the time series for 20 brain regions provides a visualization of how those regions' activities change during the entire scanning session. Therefore from these time series data, variances or covariances between different regions can be identified. Equally this give the idea about how parts of the brain communicate or work with one another, both in rest and task-based scans.

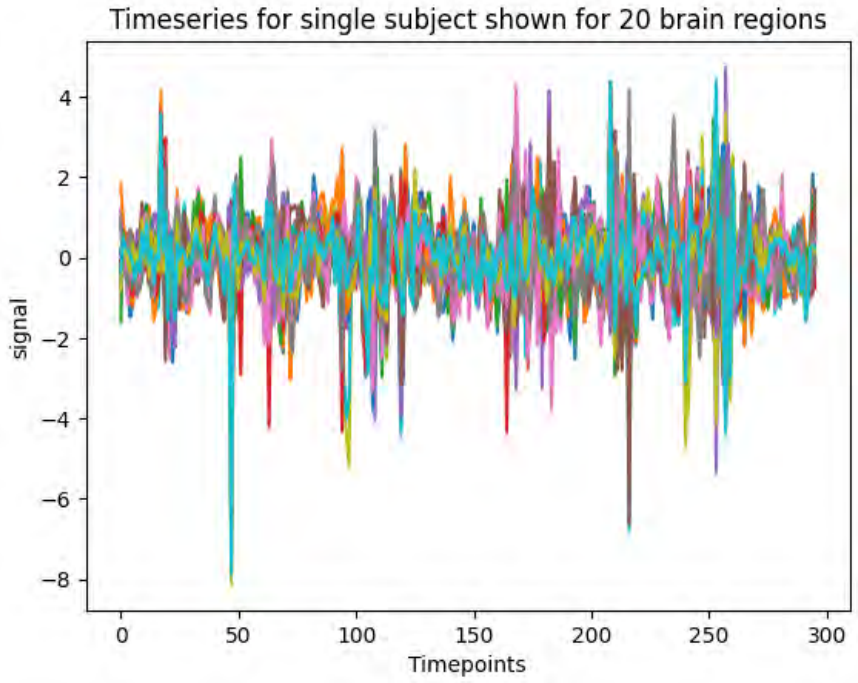

Figure 4.10: Time series for single point shown for 20 brain region

Connectivity Analysis

The Connectivity Measure function has been used object to compute the correlation matrices from the extracted time series of our ABIDE dataset. This analysis helps us understand the functional connectivity between different regions(116) of the brain. The connectivity matrix of any subject actually highlights the strength of correlation between the fmri brain regions. This matrix is a crucial feature set for training models as it summarizes the inter-regional connectivity patterns of the regions.The connectivity matrix of a random subject has been depicted in the Figure 4.11.

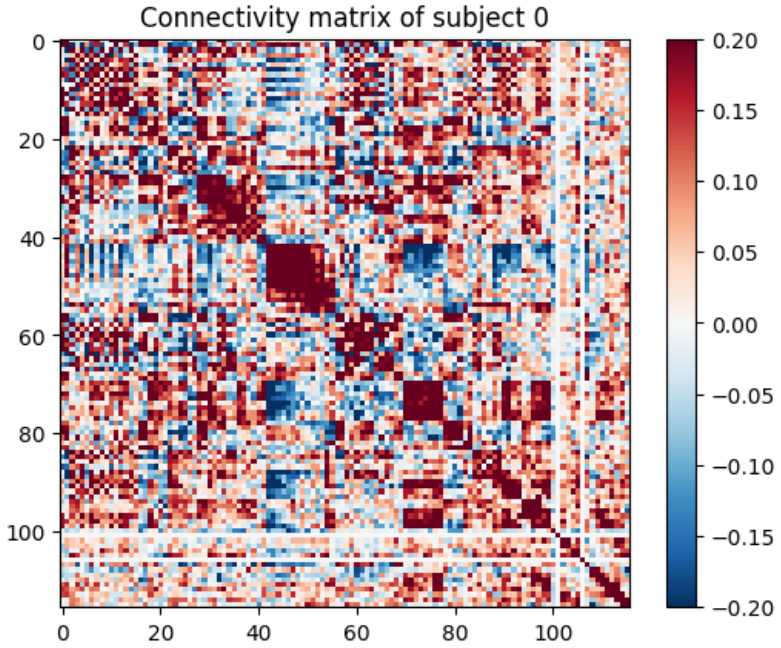

Figure 4.11: Connectivity matrix of subject 0

Correlation Matrices:

The correlation matrix for a single subject has depicted in Figure 4.12. These represent the correlation matrices of a set of matrices quantifying functional connectivity between pairs of different brain regions for several subjects from the ABIDE dataset. Each matrix will be constructed based on time series data obtained with functional MRI, or fMRI, in which the activity of the brains for each subject is recorded as a function of time. In these matrices, every entry stands for the correlation coefficient between pairs of brain regions and reflects how well the activity level is synchronized. A positive correlation suggests that in both regions, the activity goes up or down together, while a negative correlation suggests that whenever one region shows increased activity, the activity of the other region decreases. For the ABIDE dataset the DX_GROUP with the value of 1 or 0 field refers to the diagnostic group of each subject. It indicates whether the subject is part of the autism spectrum disorder (ASD) group or the neurotypical (control) group. Specifically.1 indicates that the subject is diagnosed with Autism Spectrum Disorder (ASD). Again 2 indicates that the subject is a neurotypical (control) individual, meaning they do not have ASD. The correlation matrices visually plotted the dataset using the plots that are displayed in figure and figure. This showing the differences in brain connectivity between ASD and non-ASD groups, provided by the 116 regions of the brain as determined by the AAL-Atlantis Automated Anatomical Labeling atlas: 90 cortical regions including 45 for the left hemisphere and 45 for the right hemisphere, and 26 cerebellar and subcortical regions such as the cerebellum and vermis. This will provide a fine-grained analysis of the patterns of functional connectivity related to ASD compared to neurotypical development.

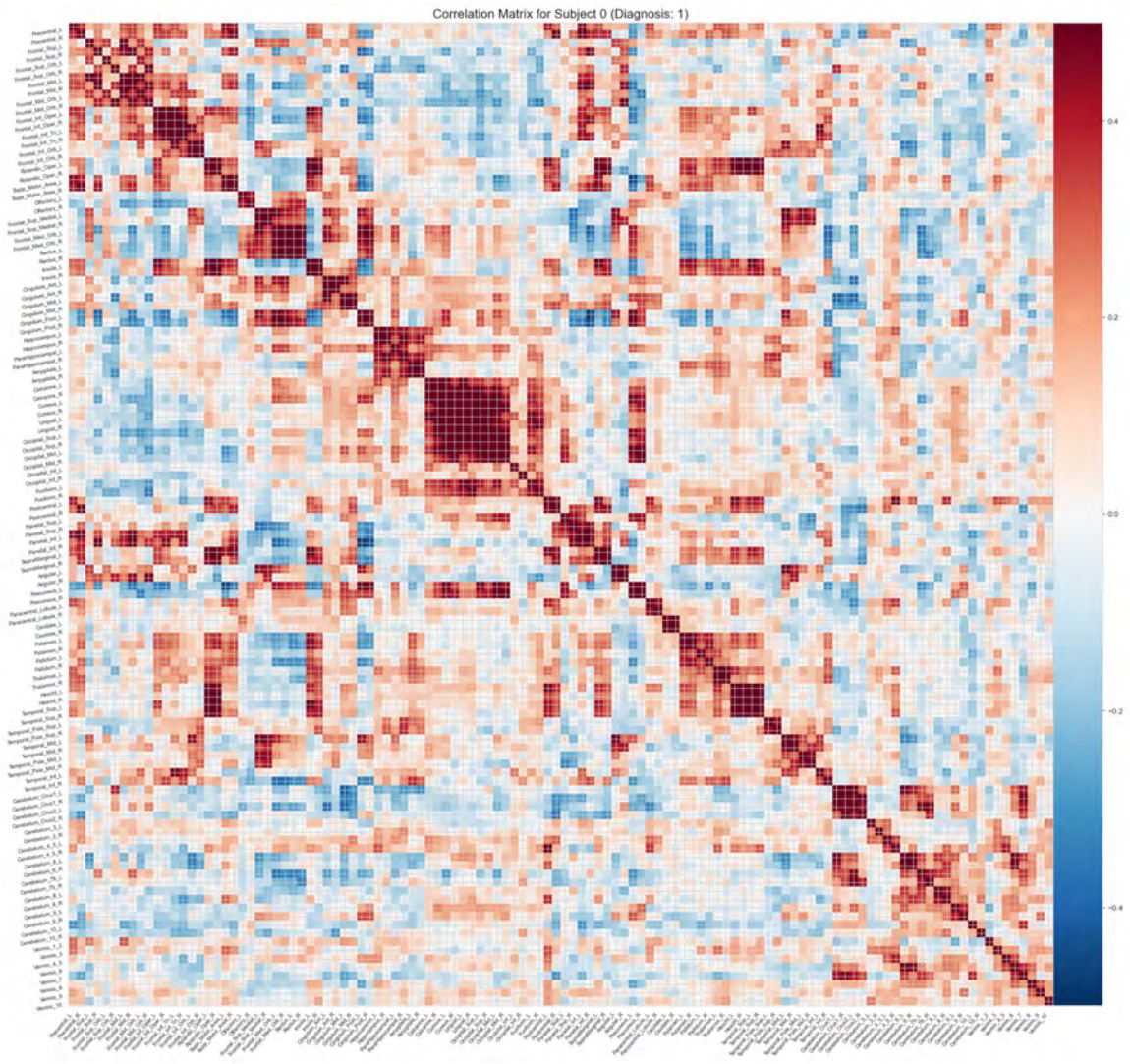

Figure 4.12: Correlation Matrix for Subject n Diagnosis as ASD

For the ABIDE dataset the ASD and and Non ASD has been labeled as 1 and 2 consecutively.

4.3.3 Model Training

LSTM Model: Firstly the Long Short-Term Memory (LSTM) networks has been trained on the extracted data from both Dosenbach Atlasand AAL atlas. As LSTM is suites for processing the sequential data, this model were implemented to exploit the time series from the fMRI scans, where at each time stamp multiple regions of the brain activities have been recorded. Thus this becomes important in learning temporal dependencies that are associated with ASD in the patterns of activity in brains. Moreover, to avoid overfitting, dropout layers were added so that the model was able to generalize well to the data it would not have seen. This is because the recurrent structure of LSTM allowed it to learn both short- and long-term temporal patterns present in brain connectivity.

BiLSTM Model: BiLSTM networks were implemented to further refine the temporal dependency modeling. This extends traditional LSTM by processing input

sequences in both forward and backward directions. This bidirectional flow enables the model to capture temporal relationships based on past information as well as by anticipating future states. This perspective ensures that the model is geared toward the learning complex as well as ensures the multi-faceted interactions across time between brain regions for enhanced ASD classification performance.

GRU Model: Utilized Gated Recurrent Units (GRU) to enhance computational efficiency while maintaining performance. This is a type of LSTM that tries to model the temporal dependencies of the input in a much more efficient way using fewer parameters. It is trained on sequential fMRI time series data, modeling how the activities across different brain regions evolve over time, not unlike the LSTM. It's gating mechanisms control the flow of information in the network, allowing GRU to have a good tradeoff between the efficiency of learning and accuracy. Attention to important patterns in a time series let GRU capture subtle temporal dynamics relevant for ASD detection but be computationally faster and lighter compared to the LSTM architecture.

DNN Model: A deep neural network is trained on the flattened functional connectivity matrices that were derived from fMRI data using AL atlas. These matrices contain the statistical correlations between different brain regions and give a sort of abstract representation of inter-regional connectivity. This architecture of DNN used fully connected layers to process these high-dimensional matrices and learned complex patterns that distinguish ASD from non-ASD subjects. Besides all these its input has shown remarkable efficacy, underlining the predictive power of functional connectivity as a biomarker for ASD.

CNN Model: Convolutional Neural Networks (CNN) has been trained to analyze spatially structured correlation matrices. This is used to examine the correlation matrices obtained from the fMRI studies as representation of the functional connectivity between different brain regions. In this respect, the Frontal and Temporal lobes were included because previous studies identified them as significant in ASD. These CNN convolutional layers capture the spatial dependencies and local patterns in the brain, thereby leveraging the natural structure from the correlation matrix for enhancing ASD classification.

GCN Model: The GCN model is designed to classify nodes or graphs based on their structural and feature information. This model performs binary classification, predicting whether a sample belongs to one of two classes. The early stopping has been used to avoid overfitting by halting training when validation loss stops improving. Besides the implementation of model checkpointing ensures the best-performing model is saved during training. Again the dropout and L2 regularization improve generalization by mitigating overfitting/ Which helps in Capturing both local and global connectivity patterns of the brain. Leverages graph-structured data to improve classification performance. Can generalize well when properly trained and validated.

Ensemble Model:
Combine LSTM and GRU outputs using adaptive weighting to form the ensemble model,leveraging spatiotemporal sequence learning for ASD classification. Specially

this ensemble approach is designed to optimize performance of efficiency through strategic model integration, leveraging each model's strengths. This helps in achieving better classification accuracy.

Model Optimization and Validation
The optimization process is rigorously structured, involving advanced techniques such as Adam optimizer for tailored learning rate adjustments and binary cross-entropy for loss optimization. Performance stabilization is ensured through early stopping and model checkpointing, safeguarding against overfitting and ensuring model robustness.

Evaluation Metrics and Further Validation
The model undergoes a thorough performance evaluation to ascertain its robustness and efficiency. Integration of Hyperparameter tuning, facilitated by tools like Optuna, has been used to refine the models to peak performance. The final step of the approach involves meticulous validation and testing. This ensures that the models not only perform optimally in a controlled environment of training but generalize well to new, unseen datasets. This thus-constituted methodological framework is representative of cutting-edge approach for neuroimaging analysis and aspires to appreciably raise the diagnostic accuracies with a further step in computational intelligence and deep learning sophistication.

4.3.4 Constraints of the Initial Approach

Our initial approach leveraged atlas-based segmentation and sequential models, but is really hampered by several critical limitations that make it hard to deal with the intricacies of the spatiotemporal features in fMRI data completely. So we shifted and developed a 3D-CNN based model that overcomes these lacunae and hence offers a wider choice for ASD classification. Following are the key justification for shifting toward different approach

1. **Loss of Spatiotemporal Granularity:**
    - Atlas-based parcellation reduces the spatial resolution by aggregating voxel-level data into predefined ROIs, potentially missing fine-grained spatial patterns critical for ASD classification.
    - Sequential models like LSTM and GRU excel in temporal modeling but fail to directly capture spatial dependencies inherent in fMRI data.
2. **Subjective Feature Engineering:**
    - The reliance on mentioned ROIs and correlation matrices imposes bias, has limited the model's capacity to autonomously learn complex and emergent patterns throughout the brain.
    - Summarization techniques can obscure higher-order spatiotemporal interactions.
3. **Computational Inefficiency:**

- Sequential models, particularly BiLSTM and GRU, are computationally intensive, requiring substantial resources to process high-dimensional fMRI time-series data.
- Ensemble techniques proposed initially, although has improved the robustness, has added another layer of computational overhead, especially when scaling across datasets.

4. **Data Sparsity:**

   - With limited sample sizes less than 200 subjects typical in fMRI datasets, overfitting becomes a significant risk in sequential architectures, which inherently require more data to generalize effectively.

5. **Limited Hierarchical Feature**

   - Models like LSTM, GRU, and DNN lack the capability to learn hierarchical spatial representations, which are essential for understanding multi-scale neural connectivity patterns.

4.4 Final Approach and Model Specification

4.4.1 Top level Overview

The present work has developed and proposed a framework for classifying Autism Spectrum Disorder directly from 4D fMRI data. NeuroSeg3D preprocessed the data through temporal segmentation, spatial normalization, and augmentation. For the core model CASD-Net, it is designed to be a 3D Convolutional Neural Network that aims at capturing both spatial and temporal features from the fMRI data. Various techniques have been applied on this model including early stopping and learning rate scheduling. For the performance evaluation, accuracy, precision, recall, F1-score, and confusion matrices will be used. This framework offers a high-performing and interpretable solution for ASD classification directly from the Spatio-Temporal data. The workflow in Figure 4.13 demonstrated the overall final approach.

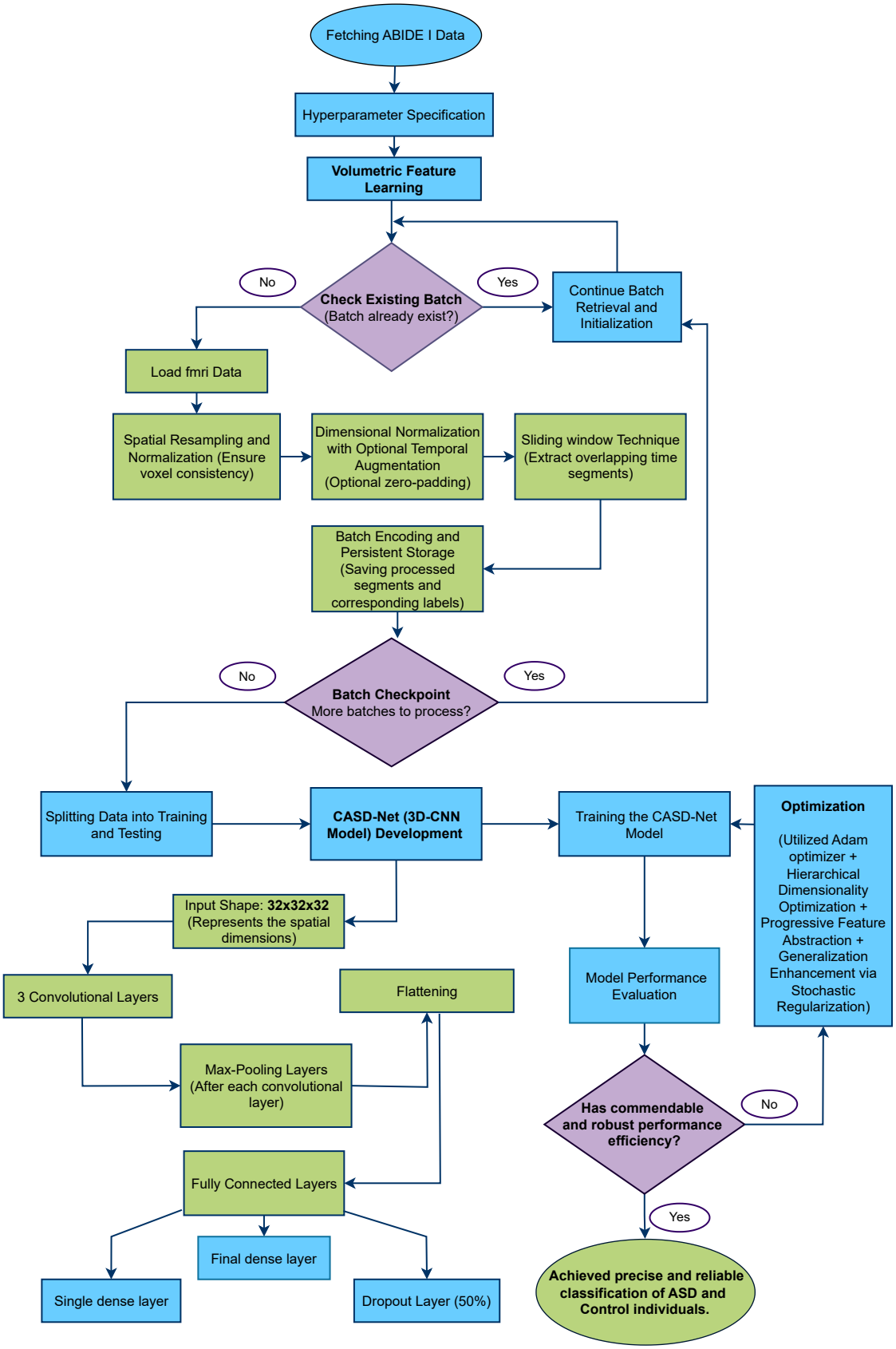

Figure 4.13: Final Approach

4.5 Data Pre-Processing

The implementation of our newly proposed NeuroSeg3D technique

4.5.1 Resampling Process:

The resampling of fMRI data is a component of the preprocessing pipeline, particularly for spatio-temporal datasets. As it often originates from different subjects with varying spatial resolutions or sizes. To resolve this issue, the pipeline ensures that all fMRI images are spatially standardized to a fixed resolution, ensuring that each image occupies the same dimensional space across all subjects, despite inherent differences in their original spatial dimensions. The resampling process allows for precise transformation of the fMRI data into a consistent format.

Target Shape: The target_shape parameter has been defined to set the desired resolution (spatial dimensions) for all fMRI images. This resolution is fixed for all subjects to guarantee uniformity across the dataset (e.g., target dimensions target_shape = (64, 64, 64) or (32, 32, 32). In our case the target shape is set to (32, 32, 32) that is data is resampled to have a consistent voxel grid of $32 \times 32 \times 32$, regardless of the original shape of the data. Moreover, this interpolates the voxel values from the original dataset (which could have a different resolution) to the new target grid using interpolation techniques such as nearest-neighbor, linear, or cubic interpolation.

Affine Transformation: The affine transformation (`original_affine`) on the other hand is a critical component in resampling, as it represents the spatial orientation and positioning of the data. It preserves the spatial integrity of the data during the resampling process, ensuring that the transformed image retains its original alignment in 3D space. Besides mapping the original affine transformation to the new space to maintain spatial consistency.
This resampling process guarantees that all fMRI images are aligned in the same spatial coordinate system, making them compatible for further analysis, regardless of their original resolution.

4.5.2 Dynamic Overlapping Temporal Segmentation

This is a dynamic temporal window segmentation process, which is applied to the total time points of each fMRI data for time-series segmentation. The segmentation process uses a sliding window to break the data into smaller segments, where each segment represents a fixed number of time points, and these segments are extracted from the full time series with overlap.
Firstly, the segment size has been defined as how many time points are included in each segment. In this research, 10 time points per segment have been used. Then, the step size has been set to 5 to determine how much the window shifts for the next segment. A step size of 5 means the window moves by 5 time points each time. As demonstrated in Figure 4.14, target shapes are resampled to a specific 3D shape for spatial consistency across all data.

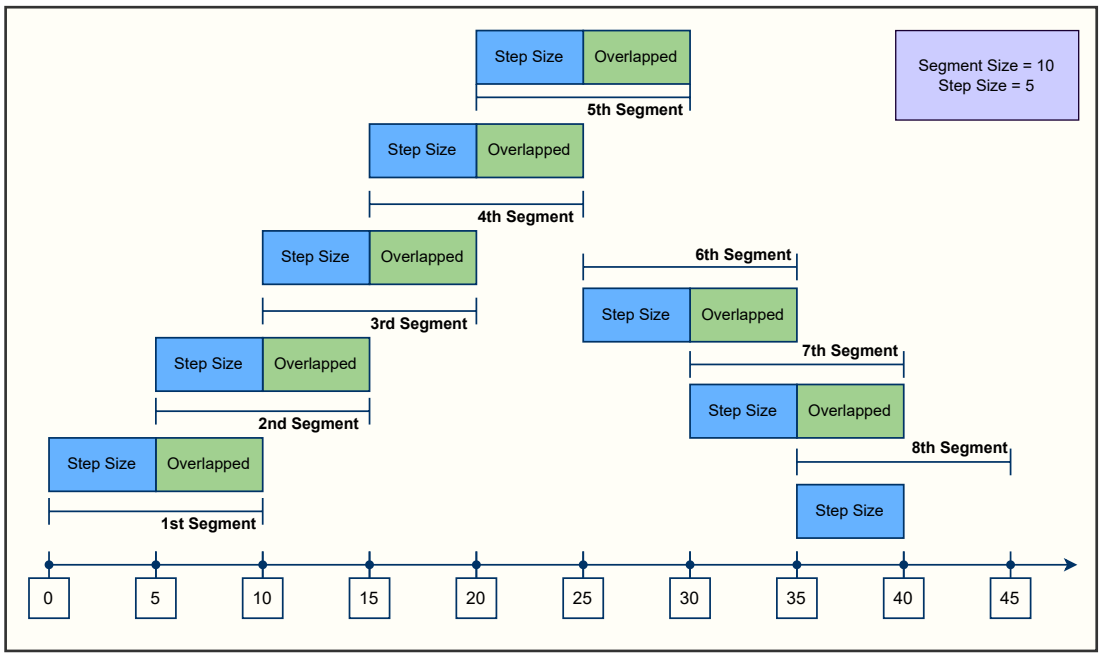

Figure 4.14: Displaying the 4D Brain Slice

Figure 4.14 provides a general visualization of the segmentation technique. For example, the first segment is extracted from time points 0 to 10, the second segment is extracted from time points 5 to 15, the third segment from time points 10 to 20, and so on.

Sliding Window Technique and Segmentation Computation

The technique is implemented by dividing the entire fMRI time-series data into smaller overlapping segments. The sliding window approach is applied dynamically, meaning it adapts to the total number of time points available for each subject or dataset. The overlap between segments ensures that no time-series data is missed, allowing for better continuity in downstream analysis.

- Firstly, the segment size (`segment_size`) is defined, determining how many time points are included in each segment.
- For each starting time point, a segment of length `segment_size` is extracted. The sliding window moves forward by `step_size` until the end of the time series is reached.
- This segmentation technique is dynamic, ensuring it works across subjects with different total time points without modifying the data.
- Overlap, controlled by `step_size`, ensures critical temporal information at segment borders is preserved. This is crucial for fMRI data, where transitions between brain states can be subtle and easily missed with disjointed segments.

To calculate the number of segments, the following equation is used, where T_{fMRI} represents the total number of time points for each subject, segment_size is the size of each segment, and step_size is the step by which the window moves:

$$Num\_of\_segments = \left\lfloor \frac{T_{fMRI} - segment\_size}{step\_size} \right\rfloor + 1 \tag{4.1}$$

Implications of the Dynamic Segmentation
This segmentation technique addresses challenges in processing 4D fMRI data of ASD and control groups while ensuring the temporal and spatial characteristics of the data are preserved for robust downstream analysis. Key benefits include:

- **Adaptation to Variable Time Points:** Dynamically adjusts to the total number of time points for each subject, ensuring compatibility across datasets with diverse temporal lengths.
- **Enhanced Temporal Resolution:** Overlap between consecutive segments ensures critical transitions in brain activity are captured.
- **Integration with Spatial Resampling:** Ensures consistency in both temporal and spatial dimensions, making the method ideal for machine learning models.
- **Generalizability:** Handles both temporal variability and spatial standardization, making it adaptable to diverse datasets from multiple sources.

4.5.3 Padding the Temporal fMRI Data

Padding mainly ensures that the temporal dimension of fMRI data is divisible by the mentioned segment size, enabling seamless extraction of uniform, complete segments and avoiding data loss at dataset edges.

Padding Calculation Formula

$$padding\_needed = (S - (T \mod S)) \mod S \tag{4.2}$$

Here, T is the total number of time points in the fMRI data and S indicates the temporal size of each segment.
The modulo operation calculates the leftover time points (R) after dividing T into complete segments. Padding ensures these leftover points form a complete segment. If $R = 0$, no padding is applied.
Padding ensures no temporal information is lost due to non-divisible time point which preserves the temporal continuity. Also, it standardizes the temporal dimension, enabling batch processing for machine learning models that helps to keep the consistency across the subjects. Moreover, it facilitates straightforward segmentation without errors related to partial segments.

This meticulous approach ensures robust data preparation, aligning with the high precision required for fMRI analysis in advanced neuroimaging studies.

4.5.4 Batch Processing and Cache Management

The most salient feature of the NeuroSeg3D pipeline is its batch processing method, allowing for scalable processing and therefore extreme memory economy by reducing data fragments to manageable pieces. The process_data_in_batches function orchestrates this by iterating through the list of fMRI image paths, ensuring that data is processed in discrete batches of a size defined by the batch_size. Initially the batch size is set to zero.

The total number of batches is calculated as:

$$\text{total\_batches} = \left\lceil \frac{\text{total\_subjects}}{\text{batch\_size}} \right\rceil$$

Here the total_subject is 613 for this research. Beside the batch size indicates the number of subjects or data samples processed together in one iteration during data processing or model training. It defines how much data is loaded into memory and used simultaneously. Again to ensure that all subjects are accounted for in the batching process, including any partial or leftover batches. This approach is critical for handling datasets that may not perfectly divide into equal batches. This is calculated as :

$$\text{total\_batches} = \left\lceil \frac{N}{B} \right\rceil$$

Here N indicated the length of the fmri path which is the total number of subjects or data points. And B indicates the batch size.

Batch Loading Process:

The batch loading process begins with a cache management system designed to reduce redundant computations by checking for previously processed batches. This process is crucial because reprocessing batches that have already been computed always waste the valuable computational resources and time. Preemptive Caching: The concept of caching ensures that, once a batch has been processed and stored, the same batch does not need to be recalculated. When the system encounters a batch that has already been processed, it loads the existing data directly from disk, effectively bypassing the resampling, padding, and segmentation steps. This `X_batch` variable holds the feature data for each subject in the batch. It contains the processed fMRI data that has undergone resampling, padding (if necessary), and segmentation. After segmentation and resampling, `X_batch` contains the feature data that will be used for downstream analysis, such as model training or statistical analysis. Again the `X_batch` represents the label data for each subject in the batch. By checking both the `X_batch` and `y_batch` files exist for a particular batch, the system ensures that data is not reprocessed. If the batch is already available, it loads the data from disk, thereby reducing computation time during later stages of analysis. The label for all segments of a subject is calculated as:

$$extended\_labels = [label] \times S \tag{4.3}$$

Here S indicates the number of each segment.

Importance of Each Step:

- **Batch Processing:** Efficiently handles large datasets, making the process memory-efficient and scalable.
- **Cache Management:** Saves computation time by ensuring that previously processed batches are reused, eliminating redundant operations.
- **Feature and Label Alignment:** This also ensures that the correct labels are associated or aligned with each data point. This is crucial for or proposed supervised learning framework.
- **Substantial Increase in Speed:** This system avoids redundant calculations by reusing this pre-processed data, substantially speeding up further processing or review stages.

Each of these steps is very important to ensure that the pipeline will process the large-sized fMRI datasets with efficiency while keeping the accuracy and reproducibility of the analysis high.

Chapter 5

Development of the CASD-Net Model for NeuroSeg3D

5.1 Architectural Pillars of CASD-Net

The architecture of the CASD-Net (Children ASD Neural Network), a developed 3D Convolutional Neural Network (CNN) proposed in this study, is designed with the intent of addressing the highly complex and multidimensional nature of fMRI data, where spatial and temporal information are both critical. The model that we developed to fit the spatio-temporal data according to the NeuroSeg3D pipeline, leverages the inherent capabilities of CNNs to capture local spatial patterns, while adapting these principles to the 3D structure of the data, enabling it to handle the volumetric and time-series aspects of fMRI effectively. The overall architecture of our model has been demonstrated in Figure 5.1 portrays the performance of the classification model in precision, recall and F1-score for two classes such as- Class 0 and Class 1. The precision is depicted by the blue bars in the chart, whereas recall is presented using light blue bars, suggesting that the model captures almost all positive samples. As F1-score is represented by the orange bar, this validates that the performance between precision and recall was balanced. Overall, this graph illustrates a well-performing model with balanced merices across both classes. Here, Precision, recall and F1-score remains at 0.94, which indicates the excellence of the model in predictive capabilities and identifying both classes accurately with minimal error.

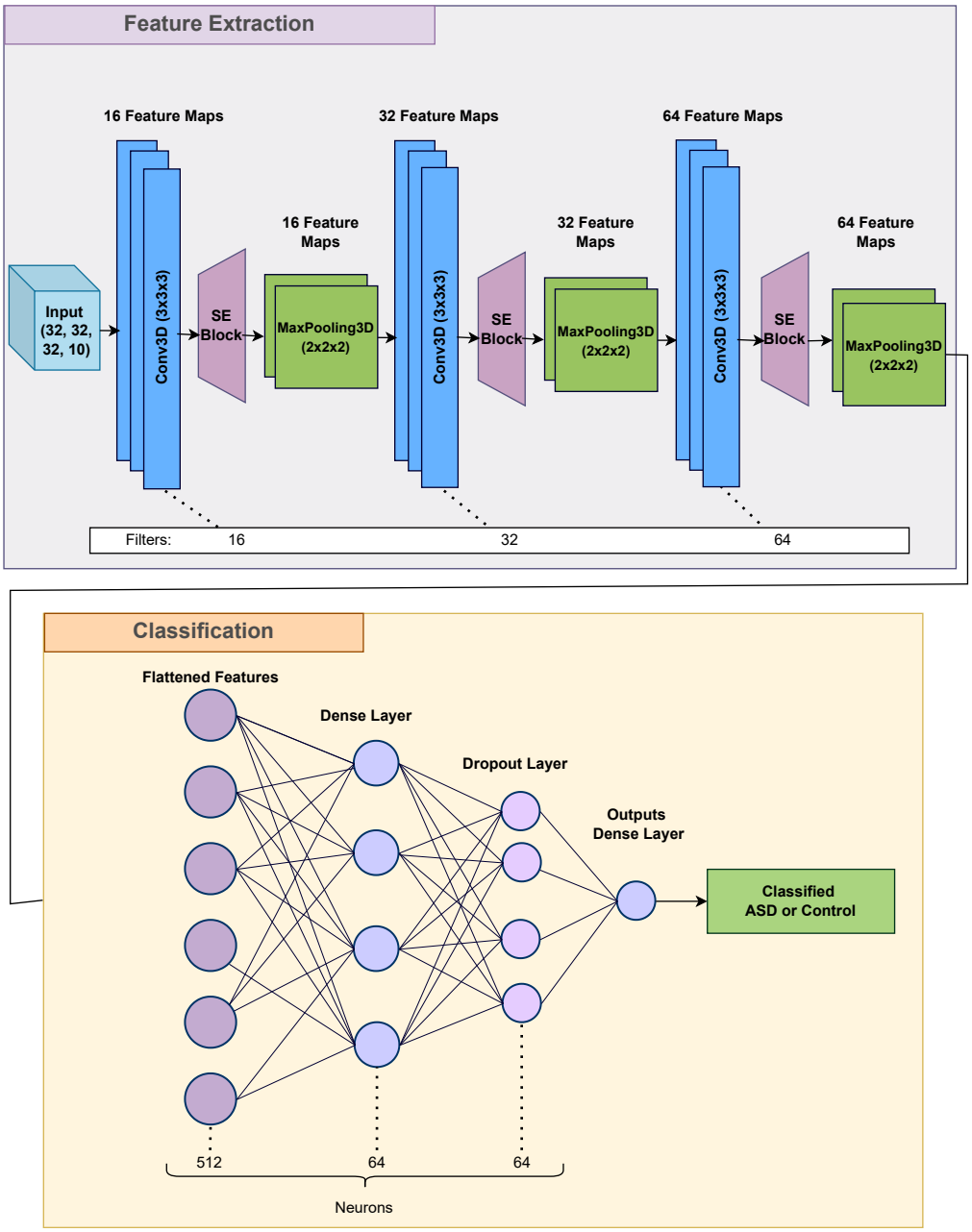

Figure 5.1: Architecture of CASD-Net(Children ASD Neural Network))

Input Shape and Data Representation: The input shape for the model is defined as (32, 32, 32, 10), which corresponds to 32x32x32 voxels (representing the spatial dimensions of the fMRI brain images) and 10 time points. This structure of the input shape reflects the nature of the 3D data and includes both spatial and temporal features, with 10 being the number of time points per segment. The inclusion of the time dimension in the input shape signifies that the model will process a sequence of frames (slices of brain activity), allowing it to capture temporal dynamics in addition to spatial relationships.

First Convolutional Layer (Conv3D): The first convolutional layer operates on the 3D data (spatial volume), where each 3D filter has a kernel size of (3, 3, 3). This shows that the filter spans a small cube of 3x3x3 voxels within the input. Especially at this stage, the low-level spatial features are extracted from the 3D

fMRI data, such as voxel-wise intensity patterns in a specific spatial region of the brain. Additionally, the ReLU activation function here introduces non-linearity that allows the model to capture complex relationships in the brain activity patterns that are crucial for distinguishing ASD from controls. This function also enables a non-linearity in the model, that enables learning capacity of complex patterns more accurately. Since fMRI data often contains noisy or weakly structured patterns, convolutional layers help enhance local coherence by learning localized features in spatial dimensions. The first convolutional layer uses 16 filters. Each filter in this stage has been designed to capture different features or patterns in the input fMRI data, such as edges, textures, or other low-level features. After this layer, the output shape is (None, 30, 30, 30, 16), where the spatial dimensions are reduced by 3 in each direction due to the 3x3x3 kernel, but the number of channels (filters) increases to 16.

First Squeeze-and-Excitation (SE) Block: The Squeeze-and-Excitation (SE) block applies Global Average Pooling (GAP), reshaping and learning channel-wise attention, but it does not change the spatial dimensions. The output shape remains (30, 30, 30, 16). This block recalibrates the learned feature maps by applying global context-awareness. This mechanism is specially very crucial for fMRI data, where certain regions may have stronger or may have weaker signals, making some features more relevant for ASD classification than others. Here, the Global Average Pooling (GAP) aggregates the features from all spatial locations to produce a single value per channel, representing the global spatial context of the input data. Additionally, the channel-wise importance is adjusted through two fully connected layers (a bottleneck layer for dimensionality reduction and an expansion layer that maps back to the original number of channels), resulting in a channel-wise attention map. The output of this SE block recalibrates the original feature map by multiplying it with the attention map, ensuring that more informative features (related to ASD differences in brain connectivity or activity) are amplified.

First Max-Pooling Layer (MaxPooling3D): This layer performs downsampling on the feature map produced by the previous convolutional layer, reducing the spatial dimensions by a factor of 2 in each direction. This reduction is achieved by taking the maximum value in each 2x2x2 spatial window, helping the model retain only the most salient features while reducing computational complexity. After max-pooling, the output shape becomes (None, 15, 15, 15, 16). The spatial dimensions are reduced, but the number of channels remains the same at 16. The max-pooling layer has no learnable parameters, so the number of parameters is 0. Moreover, pooling serves to reduce computational complexity by downsampling the features, retaining only the most significant patterns. For 4DfMR data, this pooling operation helps to abstract spatial details, allowing the model to focus on global brain activation patterns rather than fine-grained voxel-level details. Beside this it also provides some level of translation invariance, meaning that the model becomes less sensitive to small shifts in the brain regions represented in the data.

Second Convolutional Layer (Conv3D): This layer is similar to the first convolutional layer but with 32 filters instead of 16. The increase in the number of filters in this layer allows the model to capture more complex patterns as well as higher-level features from the downsampled data. The kernel size remains (3, 3, 3),

and the ReLU activation function continues to enable the model to learn intricate, non-linear patterns. The output of this layer is (None, 13, 13, 13, 32) after the convolution operation, which results in a slight reduction of the spatial dimensions, but an increase in the depth (number of filters) to 32. Additionally, the second convolutional block expands the depth of the feature maps, using 32 filters to extract more complex, high-level spatial features that are indicative of ASD-related differences in brain structure or function. The deeper convolutional layers have the task to capture larger receptive fields, meaning that they are sensitive to broader regions of the brain, incorporating more complex correlations between different brain areas.

Second Squeeze-and-Excitation (SE) Block: The second SE block recalibrates the newly learned feature maps. This mechanism plays an important role throughout the model, especially when we are dealing with the 4D data like fMRI, where different regions or times may have varying levels of relevance for the classification task. In addition, application of the SE block diverts the focus attention on the most important features that are likely to correspond to ASD-related brain activity patterns.

Second Max-Pooling Layer (MaxPooling3D): The second max-pooling layer further reduces the spatial dimensions by half in each direction, bringing the output shape to (None, 6, 6, 6, 32). Integrating this step allows the model to retain only the most essential features from the previous layer while dramatically reducing the number of parameters in subsequent layers. The max-pooling layer has no learnable parameters, so the number of parameters is 0.

Third Convolutional Layer (Conv3D): This layer uses 64 filters with a kernel size of (3, 3, 3), significantly increasing the capacity of the model to learn high-level patterns from the data. After the convolution operation, the output shape is reduced to (None, 4, 4, 4, 64). This reduction in size results from the convolution operation and the reduction in spatial resolution from the previous pooling layers.

Third Squeeze-and-Excitation (SE) Block: The final SE block refines the model's understanding of the learned feature maps by recalibrating the importance of different channels. This enables the model to emphasize the most relevant brain regions or temporal features that are indicative of ASD.

Third Max-Pooling Layer (MaxPooling3D): The final max-pooling layer reduces the spatial dimensions further, resulting in an output shape of (None, 2, 2, 2, 64). By this point, the spatial dimensions have been greatly reduced, and the feature maps contain high-level abstractions of the input data. The max-pooling layer has no learnable parameters, so the number of parameters is 0. Also, this layer operation reduces the spatial resolution from (4, 4, 4) to (2, 2, 2). This ensures that the model focuses on high-level abstract representations only rather than low-level spatial details. This actually ensures that the model has the capability to generalize across various complex data, which is important to deal with inter-individual variability in fMRI scans like ASD classification.

Flatten Layer: The Flatten layer converts the 3D tensor into a 1D vector. This is necessary because the fully connected layers (Dense layers) can only accept 1D input. The output is a 1D array of size 512, which represents the compressed

features from the entire fMRI volume. The flatten operation does not have any learnable parameters, so the number of parameters is 0. The Flatten layer reshapes the 3D output of the final pooling layer into a 1D vector, which is then ready for the fully connected layers. This step specially condenses the rich spatial features into a compact and meaningful vector that can capture the brain activity or connectivity patterns. For ASD classification,

Fully Connected Layer (Dense) This fully connected layer has 64 units and uses ReLU activation. It helps to further learn the high-level patterns extracted by the convolutional layers and flattening operation. This also serves as a dense, nonlinear transformation which allows the model to learn complex interactions between the extracted features. These neurons process the global brain activity learned by the convolutional layers and further refine the feature representation, making it more discriminative for ASD detection. The use of ReLU activation introduces non-linearity, allowing the model to approximate complex decision boundaries between ASD and control classes.
Dropout Layer The Dropout layer with a rate of 0.5 is added to prevent overfitting during training. For fMRI classification, where limited labeled data is often available, dropout plays a key role in improving the model's ability to generalize across unseen data and avoid overfitting to specific brain patterns that may not generalize to the larger ASD population.

Final Output Layer (Dense) The final layer is a Dense layer with 1 unit, which corresponds to the binary classification task. This is classification of ASD vs. Control. The Sigmoid activation function is used to produce a value between 0 and 1, which can be interpreted as the probability of the positive class. The output layer consists of a single neuron with a sigmoid activation function, which is suited for binary classification tasks. Here, it predicts the probability of an input sample belonging to the ASD class (vs. control). A sigmoid output is ideal for tasks where we want to assign a probability score between 0 and 1, enabling the model to make a final decision about whether a given fMRI scan is from an individual with ASD or not.

Model Compilation The model is compiled using the Adam optimizer, which adapts the learning rate during training for efficient convergence. The binary cross-entropy loss function is used for evaluating how well the model's predictions align with the actual labels (ASD vs. control), and accuracy is used as the evaluation metric. This layer-by-layer explanation as well the process depicted in fig illustrates how the CASD-Net architecture processes fMRI 4D data and uses both spatial and temporal features to classify ASD. The combination of 3D convolutional layers, Squeeze-and-Excitation blocks, and max-pooling layers allows the model to effectively capture and focus on the most relevant patterns for ASD classification, while the fully connected layers and dropout ensure robust, generalized predictions.

5.1.1 Model Summary and Parameters

The CASD-Net architecture is designed to classify ASD using 4D fMRI data through a series of convolutional, Squeeze-and-Excitation (SE) blocks, max pooling, and fully connected layers. It begins with an input layer that accepts 4D fMRI data

shaped (32, 32, 32, 10) where the dimensions correspond to spatial volume and channels (e.g., timepoints or modalities). The model progressively extracts spatial features from the data using 3D convolutional layers, each followed by a Squeeze-and-Excitation block, which recalibrates the feature maps by emphasizing informative channels. Max pooling operations are interspersed to reduce the spatial dimensions while preserving important spatial relationships. The feature maps are eventually flattened into a 1D vector, which is passed through dense layers for further feature integration. A dropout layer is included to mitigate overfitting during training. The final output layer uses a sigmoid activation function to predict a binary classification result, indicating whether the input corresponds to an ASD case or a control case. The total number of parameters in the model is 107,240, all of which are trainable, with 0 non-trainable parameters. This process has made the model fully trainable having no frozen layers. Thus ensuring flexibility and adaptability during training. The total chart of model summary has been depicted in Figure 5.2.
Mention not this model is designed to efficiently process and classify high-dimensional fMRI data. Complex spatiotemporal features can be extracted from the fMRI images directly by the model employing several convolutional layers, pooling layers, and dense layers. These features then has been applied for the binary classification tasks. While the Dropout layer enhances generalization by avoiding overfitting, the introduction of ReLU activations guarantees non-linear feature learning. In the end, the architecture works well for neuroimaging analysis because it can manage the multidimensional character of fMRI data.

```
Model: "model_10"
_________________________________________________________________________________________________
 Layer (type)                   Output Shape         Param #     Connected to
=================================================================================================
 input_11 (InputLayer)          [(None, 32, 32, 32,  0           []
                                 10)]

 conv3d_36 (Conv3D)             (None, 30, 30, 30,   4336        ['input_11[0][0]']
                                16)

 global_average_pooling3d_30 (G  (None, 16)          0           ['conv3d_36[0][0]']
 lobalAveragePooling3D)

 reshape_30 (Reshape)           (None, 1, 1, 1, 16)  0           ['global_average_pooling3d_30[0][
                                                                 0]']

 dense_84 (Dense)               (None, 1, 1, 1, 1)   17          ['reshape_30[0][0]']

 dense_85 (Dense)               (None, 1, 1, 1, 16)  32          ['dense_84[0][0]']

 multiply_30 (Multiply)         (None, 30, 30, 30,   0           ['conv3d_36[0][0]',
                                16)                               'dense_85[0][0]']

 max_pooling3d_36 (MaxPooling3D  (None, 15, 15, 15,   0          ['multiply_30[0][0]']
 )                              16)

 conv3d_37 (Conv3D)             (None, 13, 13, 13,   13856       ['max_pooling3d_36[0][0]']
                                32)

 global_average_pooling3d_31 (G  (None, 32)          0           ['conv3d_37[0][0]']
 lobalAveragePooling3D)

 reshape_31 (Reshape)           (None, 1, 1, 1, 32)  0           ['global_average_pooling3d_31[0][
                                                                 0]']

 dense_86 (Dense)               (None, 1, 1, 1, 2)   66          ['reshape_31[0][0]']

 dense_87 (Dense)               (None, 1, 1, 1, 32)  96          ['dense_86[0][0]']

 multiply_31 (Multiply)         (None, 13, 13, 13,   0           ['conv3d_37[0][0]',
                                32)                               'dense_87[0][0]']

 max_pooling3d_37 (MaxPooling3D  (None, 6, 6, 6, 32)  0          ['multiply_31[0][0]']
 )

 conv3d_38 (Conv3D)             (None, 4, 4, 4, 64)  55360       ['max_pooling3d_37[0][0]']

 global_average_pooling3d_32 (G  (None, 64)          0           ['conv3d_38[0][0]']
 lobalAveragePooling3D)

 reshape_32 (Reshape)           (None, 1, 1, 1, 64)  0           ['global_average_pooling3d_32[0][
                                                                 0]']

 dense_88 (Dense)               (None, 1, 1, 1, 4)   260         ['reshape_32[0][0]']

 dense_89 (Dense)               (None, 1, 1, 1, 64)  320         ['dense_88[0][0]']

 multiply_32 (Multiply)         (None, 4, 4, 4, 64)  0           ['conv3d_38[0][0]',
                                                                  'dense_89[0][0]']

 max_pooling3d_38 (MaxPooling3D  (None, 2, 2, 2, 64)  0          ['multiply_32[0][0]']
 )

 flatten_12 (Flatten)           (None, 512)          0           ['max_pooling3d_38[0][0]']

 dense_90 (Dense)               (None, 64)           32832       ['flatten_12[0][0]']

 dropout_12 (Dropout)           (None, 64)           0           ['dense_90[0][0]']

 dense_91 (Dense)               (None, 1)            65          ['dropout_12[0][0]']

=================================================================================================
Total params: 107,240
Trainable params: 107,240
Non-trainable params: 0
_________________________________________________________________________________________________
None
```

Figure 5.2: Overall Model Summary and Parameters

Chapter 6

Implementation and Result Analysis

6.1 Model Implementation

The CASD-Net model has been implemented using several key stages that focus on preprocessing, model construction, optimization, and mitigating challenges such as overfitting and memory constraints. Let's go step-by-step to explain how this model has been implemented:

1. **Data Splitting:** At first the data has been splitted into two distinct subsets. Where the training and validation set (80%) and the test set (20%) respectively. The test set here acts as an unseen set to evaluate the model's performance after training. From the initial training and validation set, a further split was generated that separated these sets of data into 20% for a validation set. This results in 64% of the original data used for training. 16% of the total original data used for validation.

2. **Model Optimizing:** The Adam optimizer is an adaptive optimization algorithm that adjusts the learning rate during training, allowing for more efficient [39]. This is specially effective for complex tasks offered by 3D CNNs based models, where training can be unstable and sensitive to learning rate choices. It allows the model to converge faster as well as avoid the need for manual tuning of the [38]. Hence it helps the model proposed in the paper converge more efficiently without manually tuning the learning rate. Beside this the binary cross-entropy loss has been implemented, which is standard for binary classification tasks, to measure the difference between the predicted and actual labels.

3. **Loss Function (Binary Cross-Entropy):** Binary Cross-Entropy loss is used because the classification task is binary (ASD vs Non-ASD). This loss function is standard for binary classification tasks, where the model is trained to output probabilities between 0 and 1, representing the likelihood of each class. The loss function penalizes the model based on how far its predictions are from the true labels.

4. **Overfitting Mitigation:** Given the risk of overfitting due to the relatively small dataset, we employed dropout layers with a probability of 0.5. This

specially forces the network to learn more robust features by randomly dropping the units during training, thus preventing the model from becoming too reliant on specific neurons and thereby improving its generalization. Overfitting is a concern in deep learning models, especially when there is a relatively small dataset, as is often the case with fMRI data. Dropout helps the model generalize better to new, unseen data by preventing it from memorizing the training set.

5. **Challenges and Considerations**

   - **Memory Constraints:** Another consideration was the memory requirements of training a 3D-CNN, especially with fMRI data that requires a lot of memory. We mitigated this by using smaller batch sizes and processing the data in batches to ensure that we didn't run into memory limitations during training.
   - **Interpretability:** The use of SE blocks helps improve the interpretability of the model by emphasizing the most relevant features in the fMRI data. While 3D-CNNs can be somewhat challenging to interpret directly, the attention mechanism embedded in the SE blocks gives us insight into which channels and regions of the brain the model is focusing on.

Overall, the CASD-Net model offers a powerful approach in classifying the 4D fMRI data, as it is a well-optimized 3D CNN that handles the complexities of fMRI data by using 3D convolutions, SE blocks for recalibration, dropout for regularization, and Adam optimization for efficient learning.

6.2 Result Analysis

The CASD-Net model has demonstrated a commendable result with a test accuracy of 93.97%. Beyond the accuracy, a deeper analysis of the model's classification metrics, such as precision, recall, and the F1-score depicted in Figure 6.1, provides a more clear understanding of the robustness the model. For class 0 and 1, for both case the precision score is 0.94. The high precision score indicates that the model has minimized the false positives robustly while classifying the Non-ASD cases. In practical terms, the model's predictions for Control cases are highly reliable, with very few misclassifications. The overall test loss is 0.1827, which is relatively low. This indicates that the model has a very minimal errors when making predictions, showing its ability to generalize effectively on unseen data. Also, in Figure 6.2 the high precision and recall metrics ensure that the model minimizes the risks of both false positives (incorrectly identifying ASD) and false negatives (failing to detect ASD). The balanced performance across the classes underscores that the equitable detection is critical as it has balanced behavior, minimal prediction errors, as well as the ability to handle class distribution effectively. Which also has made it a highly reliable tool for identifying ASD.

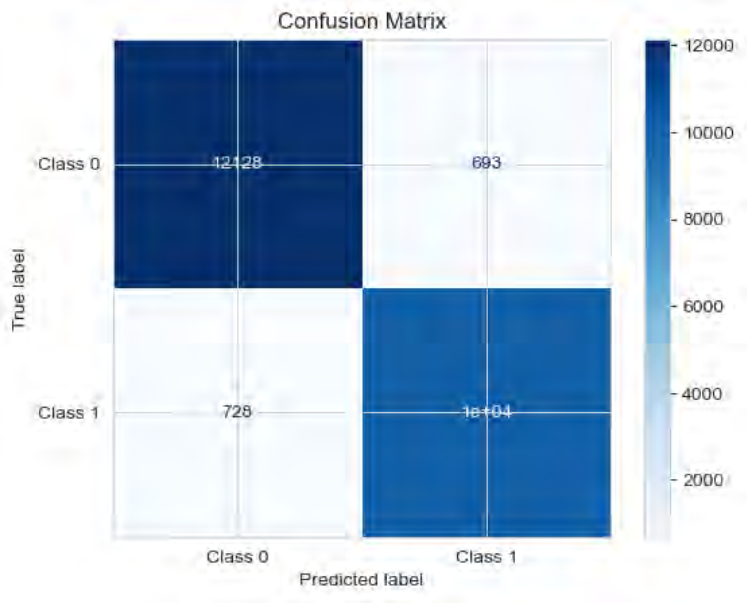

Figure 6.1: Confusion Matrix and Classification Report

Classification Report:

	precision	recall	f1-score	support
Class 0	0.94	0.95	0.94	12821
Class 1	0.94	0.93	0.93	10756
accuracy			0.94	23577
macro avg	0.94	0.94	0.94	23577
weighted avg	0.94	0.94	0.94	23577

Figure 6.2: Classification Report

6.3 Performance Analysis of the Model

In this section, we will be analyzing the performance of the model while classifying Autism Spectrum Disorder (ASD) and Controls based on 3D fMRI data. The analysis includes the evaluation metrics obtained from the model's test set as well as insights from the K-fold cross-validation process.

6.3.1 Analysis of Training and Validation Accuracy and Loss

The graphs demonstrated in Figure 6.3 depict the performance of the model in terms of accuracy and loss over 20 epochs for both training and validation datasets.

Training and Validation Accuracy

The training and validation accuracy is depicted by the left part of the graph. The training accuracy portrayed by blue lines starts at a lower value and steadily increases over the epochs. The validation accuracy in orange lines also starts at a lower value and increases steadily, closely mirroring the training accuracy. The key takeaways here are that the convergence of training and validation accuracies in the

graph mention in Figure 6.3 depicted that without significant divergence highlights that the model is learning relevant features rather than overfitting.

Training and Validation Loss

The training and validation loss is depicted by the right part of the graph in Figure 6.3. The training loss in blue lines begins relatively high which is close to 0.9 and gradually decreases across the epochs. The validation loss in orange line starts similarly high and declines consistently. The key takeaway the parallel decline in training and validation losses indicates the absence of overfitting or underfitting.The final low validation loss suggests the model has effectively learned the underlying features in the data.

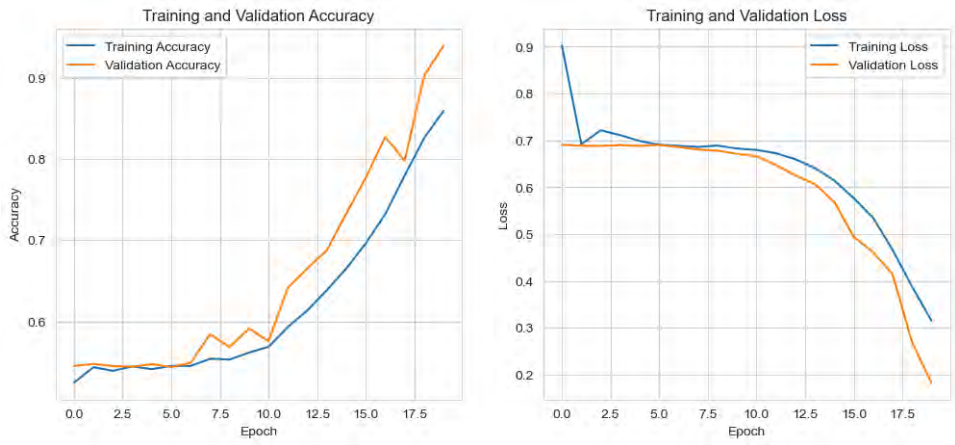

Figure 6.3: Analysis of Training and Validation Accuracy and Loss

In the graph in figure Figure 6.3 demonstrated both training and validation metrics (accuracy and loss) improve steadily over epochs, confirming a well-balanced model. The fact that validation accuracy surpasses training accuracy and validation loss decreases below training loss suggests that the model generalizes exceptionally well to unseen data. Although there is no visible gap between training and validation metrics, highlighting that the model avoids memorizing training data and instead captures meaningful patterns. The graphs also showcase a well-trained and well-optimized model. Finally validation accuracy (95%) and low validation loss suggest that the model is robust and ready for real-world testing or deployment

6.3.2 K-Fold Cross-Validation Results

To assess the model's generalizability and robustness, we performed K-fold cross-validation. The results from each fold showed significant variation, highlighting both the strengths and limitations of the model:

- **Fold 1** achieved an accuracy of 96.34% with a loss of 0.1202, which is excellent and suggests that the model performs well on the data from this fold.
- **Fold 2** showed an even higher accuracy of 98.79% with a loss of 0.0383, demonstrating that the model can perform exceptionally well under certain conditions.

- **Fold 3** had a lower accuracy of 93.63% and a loss of 0.1851, which is still solid but indicates some variability in performance.
- **Fold 4** dropped to an accuracy of 71.70% with a loss of 0.5528, showing that the model struggles with this particular subset of data.
- **Fold 5** had the lowest performance, with an accuracy of 57.38% and a loss of 0.6768, suggesting that the model encounters significant difficulty with this fold.

Despite the strong performance in some folds, the overall **average accuracy** across all five folds was 83.57%, with an average loss of 0.3147. The **standard deviation of 16.27%** in accuracy indicates considerable variability across different folds, suggesting that the model's performance may not be entirely stable across different subsets of the data.

Loss per Fold and Accuracy per Fold

The graph in Fig 6.4 represents the loss per fold as well as the accuracy per fold.

- **Loss per Fold (Left Graph)** The loss values in this model have increased consistently from Fold 1 to Fold 5, in Fig 6.4 showed an intriguing pattern, where the model achieved a very low loss of 0.1202 in Fold 1, followed by a gradual increase across the subsequent folds.
- **Accuracy per Fold (Right Graph)**

  The accuracy progression is from Fold 1 to Fold 5 in Fig 6.4. This indicates that the model achieved a very high accuracy of 98.79% in fold 2. Beside we achived accuracy over 90 % in fold 1 and 3. However in fold 4 an 5 the accuracy has degrade significantly. Although we have depicted the visualization of 5 fold. But while had run 10 fold validation the accuracy firstly has decreased gradually and after a point it started increasing. This is because the diversity and heterogeneity of our dataset.

  This demonstrates that the model is highly capable of fitting and learning from the data in the first fold, which can be attributed to the quality and representativeness of this subset. While the loss increases in subsequent folds, this is a very natural part of the training process, especially in a complex domain like 4D fMRI data. The higher loss in later folds may be due to increased complexity in the validation data, but this shows the model's ability to adapt to various data variations. Moreover the gradual increase in loss suggests that the model is exposed to different patterns and variability in the data across folds.

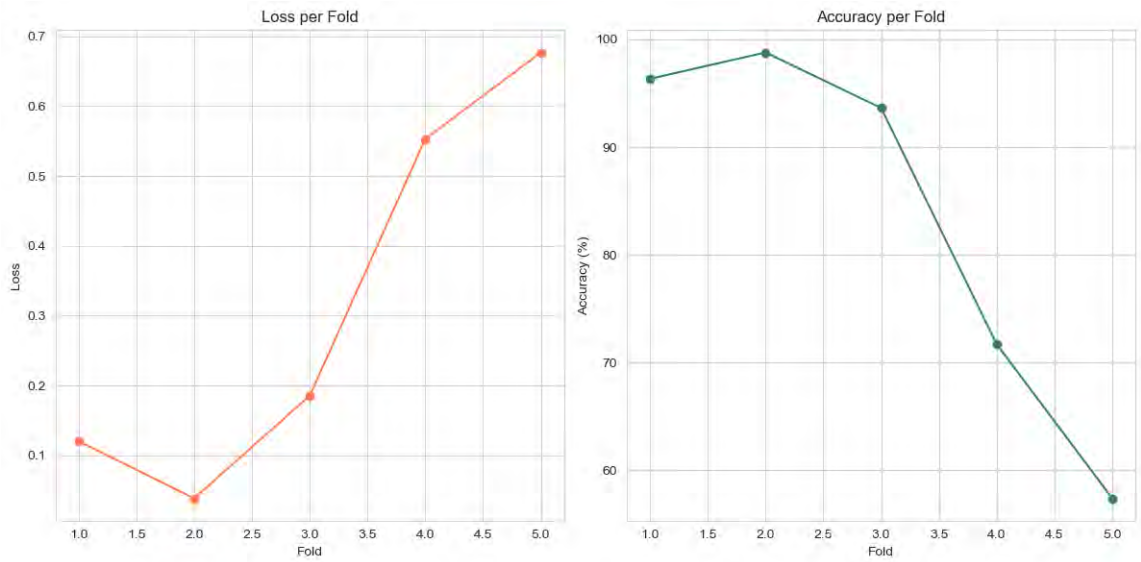

Figure 6.4: Graph Representing: Loss per Fold and Accuracy per Fold

The inverse relationship between loss and accuracy is clear in the fig. Here as loss increases, accuracy decreases. The significant performance drop between folds suggests that the model may not be robust or may be sensitive to data splits, imbalances, or noise in the validation data. If this pattern persists across multiple cross-validation runs, it would highlight a generalization issue, where the model cannot perform consistently on different subsets of data. However this does not persist across multiple cross-validation runs so the model has a robust performance.

6.4 Strengths of the Model

The bar chart in Figure 6.5 portrays the performance of the classification model in precision, recall and F1-score for two classes such as- Class 0 and Class 1. The precision is depicted by the blue bars in the chart, whereas recall is presented using light blue bars, suggesting that the model captures almost all positive samples. As F1-score is represented by the orange bar, this validates that the performance between precision and recall was balanced. Overall, this graph illustrates a well-performing model with balanced merices across both classes. Here, Precision, recall and F1-score remains at 0.94, which indicates the excellence of the model in predictive capabilities and identifying both classes accurately with minimal error.

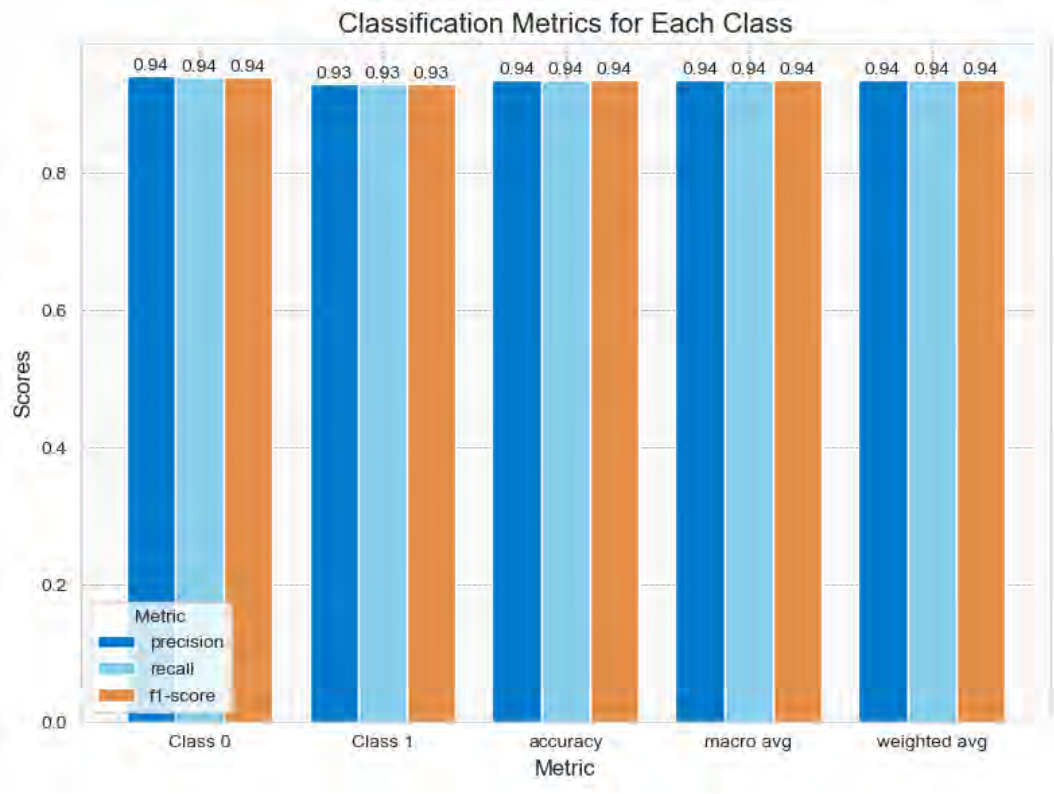

Figure 6.5: Bar chart analysis of the results

The results depict several strengths in the performance of the model.

- **High Accuracy**: As the model acquires 93.97% accuracy, this indicates the model performs strongly despite the complexity of interpreting the subtle differences in fMRI data.

- **Balanced Performance**: It can be observed that the precision and recall values for both ASD and Non-ASD classes are very close, therefore indicating that the model is well-balanced, not favoring one class over the other. This is very significant for clinical applications, as the cost of false positives and false negatives is very crucial.

- **Effective Feature Extraction**: We use 3D convolutional layers and Squeeze-and-Excitation (SE) blocks, which has been proven effective to capture both spatial and temporal dependencies of fMRI data, contributing to the ability of the model to extract relevant features that distinguish ASD from non-ASD.

Chapter 7

Conclusion

7.1 Challenges

On the way to detect ASD we came across challenges at every aspect. Our initial approach was to detect ASD in children based on their behavioral pattern. First challenge was about data collection. Due to the unavailability of clinically acclaimed data of children with ASD and lack of existing research on our topic, we looked for ways to collect data with on-field data collection. However, due to being unable to receive consent and medical validation, even after contacting professionals of various kinds who work with children with ASD, we could not collect hands-on photographic data. We then approached collecting tabular data, where we used a dataset of Dr. Fayez Thabtah with a series of yes/no questions regarding the child's behavior, such as making eye contact, pointing to objects, or responding to their name. Here, we applied various linear machine learning models to the dataset. This analysis helped to identify specific behaviors that might indicate ASD at an early stage. While the behavioral patterns provided useful insights for ASD detection, identifying the emotional state of a child from these patterns alone proved to be nearly impossible. The lack of depth in the data, particularly without access to more nuanced, real-time emotional cues like facial expressions or vocal intonations, made it difficult to reliably infer emotions. We also made an effort to collect video datasets from various schools for ASD children to enhance our analysis. However, this proved to be extremely challenging due to privacy concerns and other logistical difficulties. As a result, we were unable to incorporate video-based analysis into the project. Due to this limitation, we couldn't continue with the emotion detection aspect of the project. Despite the existing research on characteristics of ASD suggest that there could be facial indicators differentiating children with ASD from controls, the differences are so subtle that for the human eye those remain unnoticeable and through only advanced image processing techniques could be detected. After going through several trials and errors with the datasets, we finally came across the ABIDE dataset that shifted our approach to a whole different route. ABIDE being a very complex dataset itself, while working with it, retrieving 3D data with time-stamps became very complicated. Due to the size of high-dimensional fMRI data, we faced many computational errors, thus figuring out computational resources has also been a major challenge. Although we were eventually successful with our accuracy to detect ASD with our model, as we worked on the critical fMRI data, finding the best model to identify the sensitive intricacies of the data and fine-tuning the model

for achieving the best accuracy in ASD diagnosis was a major challenge in our research.

7.2 Limitation of the Research

While we came across many challenges in our approach, there are few limitations to our research as well. Due to fMRI being complex and high-dimensional data and employing deep learning models like 3D CNNs, training such models requires substantial computational power. Therefore, we met the limitation of higher computational resources. On the other hand, although high-dimensional fMRI data are very large in terms of file size, the number of subjects that we worked on is comparatively small being 613 subjects. Therefore, this limited sample size may affect the statistical power of the model, which makes it susceptible to overfitting. Moreover, the ABIDE I dataset that we worked on is a dataset of a specific demographic that is not local. As our initial approach to find data locally failed due to lack of technologically advanced repository, we were compelled to look for data outside our country, being a major limitation to our research. This leads to another major limitation of our research as this raises concerns about the generalizability of our model to other populations with different demographics. In order to ensure the model is both scalable and adaptable while working efficiently, clinical acceptability is critical.

7.3 Future Scope

With our goal to build a model using the most efficient architecture to get the best possible accuracy for us to detect ASD, our model performs successfully in that aspect. However, that also leaves room for future scope of our research in enhancing the performance of our proposed model and expanding its applicability. As we have worked with only ABIDE I dataset, our model could be implemented to both ABIDE I and ABIDE II, moreover, a larger dataset for more extensive research to detect ASD in the future. Besides, possibility in collecting native and locally sourced fMRI data could ensure the model's generalizability, as this will help the model to adapt to the cultural and demographic characteristics of our locality. Additionally, higher computational resources could help in enhancing the model's efficiency even further. In our research we only work with brain connectivity patterns using the brain signals of fMRI data, where in future we could work on finding out the behavioral patterns to diagnose the individuals with ASD. We could also use the brain signals for not only detecting the individuals with ASD, but also find suggestions for further assistance for them. Furthermore, despite CASD-Net demonstrating high accuracy, there is still scope for improving the model. Therefore, in future work, LLM could be integrated, as LLM can serve as a powerful complement to our model with their ability to process, summarize and generate natural language descriptions of complicated data. This would make ASD detection more accessible and effective to clinical practices.

7.4 Conclusion

In this paper, we propose a novel and advanced deep learning framework to acquire the best possible accuracy in detecting ASD in children and adolescents using resting-state fMRI data. In our work, we integrate NeuroSeg3D, a robust preprocessing pipeline and CASD-Net (Classification Architecture for Spatio-temporal fMRI Data) a custom 3D CNN. The architecture of this model is designed with the goal to address the highly complex and multidimensional nature of fMRI data and with our approach we effectively capture both the spatial and temporal dynamics of brain activity that we intended. While adapting the principles of the 3D structure of the fMRI data, our approach effectively handles the volumetric and time-series aspects of the data as well. In order to optimize our model CASD-Net, we have used Adam optimizer, which is particularly effective for training deep neural models like ours. For improving the model's performance further efficiently, we incorporated Squeeze-and-Excitation (SE) blocks, which recalibrates channel-wise feature responses to enhance feature representation. As we worked with complicated fMRI data with a large number of features, SE blocks helped the network in focusing on the most important features for classification. In our model, class 0 (non-ASD) had a precision of 0.94, recall of 0.95 and F1 score of 0.94, which indicates that the model is highly accurate in predicting non-ASD cases, while for class 1 (ASD) the model obtained a precision of 0.94, recall of 0.93 and F1-score of 0.93 that indicates the models high performance in identifying ASD cases as well. Moreover, for assessing the robustness and generalizability, we performed 5-fold cross-validation, where the overall average accuracy was 83.57%. Finally, the model achieved a test accuracy of 93.97% that indicates the robust performance in detecting between ASD and neurotypical controls. Although the model obtained great accuracy, there is room for further optimization to use it in broader aspects. Our future work will focus on stabalizing the model's performance across different data subsets. In conclusion, the performance of our proposed custom-designed CASD-Net demonstrates its ability to become a reliable and valuable tool for clinical applications for neuroimaging analysis in ASD diagnosis.

Bibliography

[1] C. P. Johnson, S. M. Myers, *et al.*, "Identification and evaluation of children with autism spectrum disorders," *Pediatrics*, vol. 120, no. 5, pp. 1183–1215, 2007.

[2] A. Krizhevsky, I. Sutskever, and G. E. Hinton, "Imagenet classification with deep convolutional neural networks," in *Advances in Neural Information Processing Systems*, F. Pereira, C. Burges, L. Bottou, and K. Weinberger, Eds., vol. 25, Curran Associates, Inc., 2012. [Online]. Available: https://proceedings.neurips.cc/paper_files/paper/2012/file/c399862d3b9d6b76c8436e924a68c45b-Paper.pdf.

[3] J. D. Power, K. A. Barnes, A. Z. Snyder, B. L. Schlaggar, and S. E. Petersen, "Spurious but systematic correlations in functional connectivity mri networks arise from subject motion," *Neuroimage*, vol. 59, no. 3, pp. 2142–2154, 2012.

[4] K. Cho, B. van Merrienboer, D. Bahdanau, and Y. Bengio, *On the properties of neural machine translation: Encoder-decoder approaches*, 2014. arXiv: 1409.1259 [cs.CL]. [Online]. Available: https://arxiv.org/abs/1409.1259.

[5] J. Chung, C. Gulcehre, K. Cho, and Y. Bengio, *Empirical evaluation of gated recurrent neural networks on sequence modeling*, 2014. arXiv: 1412.3555 [cs.NE]. [Online]. Available: https://arxiv.org/abs/1412.3555.

[6] Y. Lecun, Y. Bengio, and G. Hinton, "Deep learning," English (US), *Nature*, vol. 521, no. 7553, pp. 436–444, May 2015, Publisher Copyright: © 2015 Macmillan Publishers Limited. All rights reserved., ISSN: 0028-0836. DOI: 10.1038/nature14539.

[7] H. Aghdam and E. Heravi, "Guide to convolutional neural networks," *New York*, Jan. 2017. [Online]. Available: https://link.springer.com/content/pdf/10.1007/978-3-319-57550-6.pdf.

[8] R. Dey and F. M. Salem, "Gate-variants of gated recurrent unit (gru) neural networks," in *2017 IEEE 60th International Midwest Symposium on Circuits and Systems (MWSCAS)*, 2017, pp. 1597–1600. DOI: 10.1109/MWSCAS.2017.8053243.

[9] N. C. Dvornek, P. Ventola, K. A. Pelphrey, and J. S. Duncan, "Identifying autism from resting-state fmri using long short-term memory networks," in *Machine Learning in Medical Imaging: 8th International Workshop, MLMI 2017, Held in Conjunction with MICCAI 2017, Quebec City, QC, Canada, September 10, 2017, Proceedings 8*, Springer, 2017, pp. 362–370.

[10] J. Wu, "Introduction to convolutional neural networks," Jan. 2017. [Online]. Available: https://cs.nju.edu.cn/wujx/paper/CNN.pdf.

[11] J. Baio, "Prevalence of autism spectrum disorder among children aged 8 years—autism and developmental disabilities monitoring network, 11 sites, united states, 2014," *MMWR. Surveillance Summaries*, vol. 67, 2018.

[12] C. Caballero, S. Mistry, J. Vero, and E. B. Torres, "Characterization of noise signatures of involuntary head motion in the autism brain imaging data exchange repository," *Frontiers in Integrative Neuroscience*, vol. 12, 2018, ISSN: 1662-5145. DOI: 10.3389/fnint.2018.00007. [Online]. Available: https://www.frontiersin.org/journals/integrative-neuroscience/articles/10.3389/fnint.2018.00007.

[13] A. S. Heinsfeld, A. R. Franco, R. C. Craddock, A. Buchweitz, and F. Meneguzzi, "Identification of autism spectrum disorder using deep learning and the abide dataset," *NeuroImage: Clinical*, vol. 17, pp. 16–23, 2018.

[14] X. Li, N. C. Dvornek, X. Papademetris, *et al.*, "2-channel convolutional 3d deep neural network (2cc3d) for fmri analysis: Asd classification and feature learning," in *2018 IEEE 15th International Symposium on Biomedical Imaging (ISBI 2018)*, IEEE, 2018, pp. 1252–1255.

[15] M. Thomas and A. Chandran, "Artificial neural network for diagnosing autism spectrum disorder," in *2018 2nd International Conference on Trends in Electronics and Informatics (ICOEI)*, 2018, pp. 930–933. DOI: 10.1109/ICOEI.2018.8553781.

[16] Y. Zhao, F. Ge, S. Zhang, and T. Liu, "3d deep convolutional neural network revealed the value of brain network overlap in differentiating autism spectrum disorder from healthy controls: 21st international conference, granada, spain, september 16-20, 2018, proceedings, part iii," in Sep. 2018, pp. 172–180, ISBN: 978-3-030-00930-4. DOI: 10.1007/978-3-030-00931-1_20.

[17] M. N. Parikh, H. Li, and L. He, "Enhancing diagnosis of autism with optimized machine learning models and personal characteristic data," *Frontiers in computational neuroscience*, vol. 13, p. 9, 2019.

[18] C. Wang, Z. Xiao, B. Wang, and J. Wu, "Identification of autism based on svm-rfe and stacked sparse auto-encoder," *Ieee Access*, vol. 7, pp. 118 030–118 036, 2019.

[19] X. Yang, M. S. Islam, and A. A. Khaled, "Functional connectivity magnetic resonance imaging classification of autism spectrum disorder using the multisite abide dataset," in *2019 IEEE EMBS international conference on biomedical & health informatics (BHI)*, IEEE, 2019, pp. 1–4.

[20] K. Byeon, J. Kwon, J. Hong, and H. Park, "Artificial neural network inspired by neuroimaging connectivity: Application in autism spectrum disorder," in *2020 IEEE International Conference on Big Data and Smart Computing (BigComp)*, 2020, pp. 575–578. DOI: 10.1109/BigComp48618.2020.00013.

[21] R. C. Craddock, P. Bellec, D. Clark, *et al.*, *Abide preprocessed: Data from the autism brain imaging data exchange preprocessed connectomes project*, Retrieved from http://preprocessed-connectomes-project.org/abide/, 2020. [Online]. Available: http://preprocessed-connectomes-project.org/abide/.

[22] G. V. Houdt, C. Mosquera, and G. Nápoles, "A review on the long short-term memory model," *Artificial Intelligence Review*, vol. 53, pp. 5929–5955, 2020, Published May 13, 2020. DOI: 10.1007/s10462-020-09838-1. [Online]. Available: https://doi.org/10.1007/s10462-020-09838-1.

[23] X. Yang, P. T. Schrader, and N. Zhang, "A deep neural network study of the abide repository on autism spectrum classification," *International journal of advanced computer science and applications*, vol. 11, no. 4, 2020.

[24] M. S. Ahammed, S. Niu, M. R. Ahmed, J. Dong, X. Gao, and Y. Chen, "Darkasdnet: Classification of asd on functional mri using deep neural network," *Frontiers in Neuroinformatics*, vol. 15, p. 635 657, 2021.

[25] F. Almuqhim and F. Saeed, "Asd-saenet: A sparse autoencoder, and deep-neural network model for detecting autism spectrum disorder (asd) using fmri data," *Frontiers in Computational Neuroscience*, vol. 15, p. 654 315, 2021.

[26] M. A. Bayram, İ. Özer, and F. Temurtaş, "Deep learning methods for autism spectrum disorder diagnosis based on fmri images," *Sakarya University Journal of Computer and Information Sciences*, vol. 4, no. 1, pp. 142–155, 2021.

[27] T. M. Epalle, Y. Song, Z. Liu, and H. Lu, "Multi-atlas classification of autism spectrum disorder with hinge loss trained deep architectures: Abide i results," *Applied soft computing*, vol. 107, p. 107 375, 2021.

[28] J. O. Maximo, C. M. Nelson, and R. K. Kana, ""unrest while resting"? brain entropy in autism spectrum disorder," *Brain Research*, vol. 1762, p. 147 435, 2021, ISSN: 0006-8993. DOI: https://doi.org/10.1016/j.brainres.2021.147435. [Online]. Available: https://www.sciencedirect.com/science/article/pii/S0006899321002924.

[29] F. Z. Subah, K. Deb, P. K. Dhar, and T. Koshiba, "A deep learning approach to predict autism spectrum disorder using multisite resting-state fmri," *Applied Sciences*, vol. 11, no. 8, p. 3636, 2021.

[30] M. B. Ahsan Tamal, M. A. Alam, M. N. Sharker, and M. Islam Sazib, "Forecasting of solar photovoltaic output energy using lstm machine learning algorithm," in *2022 4th International Conference on Sustainable Technologies for Industry 4.0 (STI)*, 2022, pp. 1–6. DOI: 10.1109/STI56238.2022.10103310.

[31] Z. Li, F. Liu, W. Yang, S. Peng, and J. Zhou, "A survey of convolutional neural networks: Analysis, applications, and prospects," *IEEE Transactions on Neural Networks and Learning Systems*, vol. 33, no. 12, pp. 6999–7019, 2022. DOI: 10.1109/TNNLS.2021.3084827.

[32] F. Z. Benabdallah, A. Drissi El Maliani, D. Lotfi, and M. El Hassouni, "A convolutional neural network-based connectivity enhancement approach for autism spectrum disorder detection," *Journal of Imaging*, vol. 9, no. 6, p. 110, 2023.

[33] R. Cahuantzi, X. Chen, and S. Güttel, "A comparison of lstm and gru networks for learning symbolic sequences," in *Science and Information Conference*, Springer, 2023, pp. 771–785.

[34] M. Feng and J. Xu, "Detection of asd children through deep-learning application of fmri," *Children*, vol. 10, no. 10, p. 1654, 2023.

[35] MIT Media Lab, *Overview ‹ affective computing*, https://www.media.mit.edu/groups/affective-computing/overview/, [Accessed 20-09-2023], 2023.

[36] N. Qiang, J. Gao, Q. Dong, *et al.*, "A deep learning method for autism spectrum disorder identification based on interactions of hierarchical brain networks," *Behavioural Brain Research*, vol. 452, p. 114 603, 2023.

[37] A. M. Sabegh, N. Samadzadehaghdam, H. Seyedarabi, and T. Ghadiri, "Automatic detection of autism spectrum disorder based on fmri images using a novel convolutional neural network," *Research on Biomedical Engineering*, vol. 39, no. 2, pp. 407–413, 2023.

[38] L. Shao, C. Fu, and X. Chen, "A heterogeneous graph convolutional attention network method for classification of autism spectrum disorder," *BMC Bioinformatics*, vol. 24, Sep. 2023. DOI: 10.1186/s12859-023-05495-7.

[39] A. Vidhya, *What is adam optimizer?* Accessed: 2024-11-29, 2023. [Online]. Available: https://www.analyticsvidhya.com/blog/2023/09/what-is-adam-optimizer/#:~:text=The%20Adam%20optimizer%2C%20short%20for,Developed%20by%20Diederik%20P.

[40] A. Yousefian, F. Shayegh, and Z. Maleki, "Detection of autism spectrum disorder using graph representation learning algorithms and deep neural network, based on fmri signals," *Frontiers in Systems Neuroscience*, vol. 16, p. 904 770, 2023.

[41] J. Zhang, F. Feng, T. Han, X. Gong, and F. Duan, "Detection of autism spectrum disorder using fmri functional connectivity with feature selection and deep learning," *Cognitive Computation*, vol. 15, no. 4, pp. 1106–1117, 2023.

[42] I. Chkifa, A. Majda, and M. Garouani, "Exploratory abide dataset analysis for autism detection," Ph.D. dissertation, Université moulay Ismail/Ensam Meknes, 2024.

[43] A. Mahmoud and A. Mohammed, "Leveraging hybrid deep learning models for enhanced multivariate time series forecasting," *Neural Processing Letters*, vol. 56, 2024, Accessed 20-09-2023. DOI: 10.1007/s11063-024-11656-3. [Online]. Available: https://link.springer.com/article/10.1007/s11063-024-11656-3.

[44] I. D. Mienye, T. G. Swart, and G. Obaido, "Recurrent neural networks: A comprehensive review of architectures, variants, and applications," *Information*, vol. 15, no. 9, 2024, ISSN: 2078-2489. DOI: 10.3390/info15090517. [Online]. Available: https://www.mdpi.com/2078-2489/15/9/517.

[45] C. Nagamani, T. R. Devi, G. G. Babu, and V. Sindhu, "Comparative exploration of machine learning models for enhanced autism detection," in *2024 International Conference on Inventive Computation Technologies (ICICT)*, 2024, pp. 925–932. DOI: 10.1109/ICICT60155.2024.10544973.

[46] S. Yoo, Y. Jang, S.-J. Hong, *et al.*, "Whole-brain structural connectome asymmetry in autism," *NeuroImage*, vol. 288, p. 120 534, 2024, ISSN: 1053-8119. DOI: https://doi.org/10.1016/j.neuroimage.2024.120534. [Online]. Available: https://www.sciencedirect.com/science/article/pii/S1053811924000296.